Contract No:

This document was prepared in conjunction with work accomplished under Contract No. 89303321CEM000080 with the U.S. Department of Energy (DOE) Office of Environmental Management (EM).

Disclaimer:

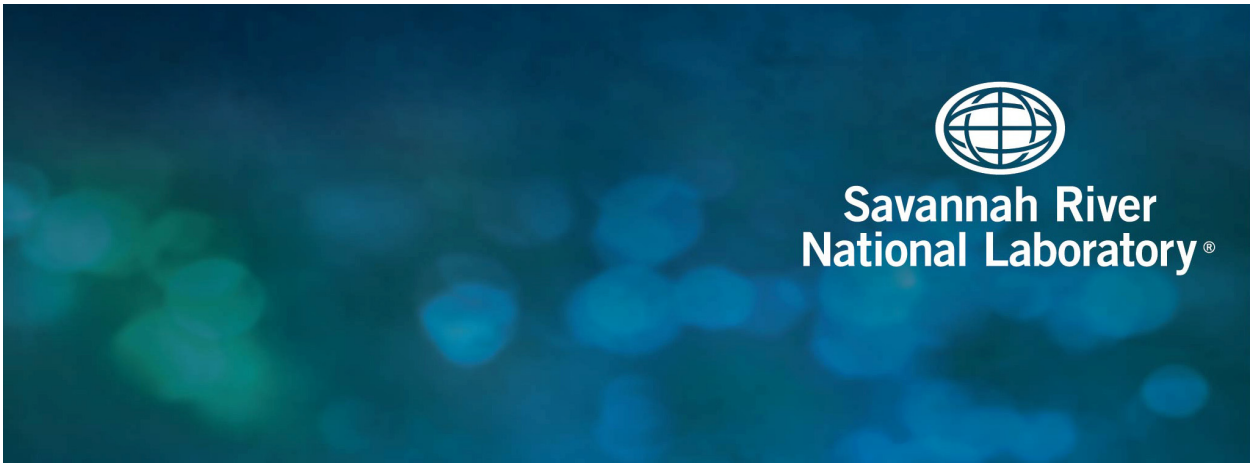

A U.S. DEPARTMENT OF ENERGY NATIONAL LAB • SAVANNAH RIVER SITE • AIKEN, SC • USA

PORFLOW Modeling of Vadose Zone Flow and Transport for the E-Area Intermediate Level Vault

F. G. Smith, III

December 2021

SRNL-STI-2020-00410, Revision 1

DISCLAIMER

Printed in the United States of America

Prepared for
U.S. Department of Energy

SRNL-STI-2020-00410
Revision 1

Keywords: *ILV, Concrete, TPBAR, Waste Disposal, ELLWF*

Retention: *Permanent*

PORFLOW Modeling of Vadose Zone Flow and Transport for E-Area Intermediate Level Vault

F. G. Smith, III

December 2021

Savannah River National Laboratory is operated by Battelle Savannah River Alliance for the U.S. Department of Energy under Contract No. 89303321CEM000080.

REVIEWS AND APPROVALS

AUTHORS:

_____
F. G. Smith, III, Environmental Science & Dosimetry, SRNL

TECHNICAL REVIEW:

_____
T. Hang, Advanced Modeling & Simulation, SRNL, Reviewed per E7 2.60

APPROVAL:

_____
J. J. Mayer, Earth & Biological Systems, SRNL

_____
M. Cofer, Manager, Environmental Science & Dosimetry, SRNL

_____
B. D. Lee, Manager, Earth & Environmental Science, SRNL

REVISION CHANGE LOG

Revision 1a March 2021	The Rev. 0 calculations used a 2.5% gravel 97.5% concrete mixture to represent cracked concrete. This was changed to a 10% gravel 90% concrete mixture to be more conservative and to agree with the composition used for LAW Vault modeling. All model calculations were redone, and results shown in Section 6 of the report and the Appendices have been changed.
	The number of time periods used in the modeling was expanded from 20 to 35. Table 5-1 and the attendant description were revised to include this change.
	Table 5-2 was revised to indicate the new initial concrete/gravel blending.
	When comparing the ILV model results to those obtained in the 2008 PA, 2008 PA results were plotted with the time shifted 70 years to align the placement of the closure cap between the two models. To avoid any confusion caused by this time displacement, comparison plots were revised so that time zero is the start of ILV operations for both models.
	Figure 4-1 was revised to show that the ILV extends into the lower vadose zone.
	Mo-93 and its daughter Nb-93m were dropped from the isotopes modeled because the K_d changed from 0 in 2008 to 1000 in the latest chemistry database. The large change in K_d made a comparison to the 2008 PA transport results irrelevant. Reference to these isotopes in Table 6-3 was deleted.
	Modeling of tritium flux to the water table originating from TPBAR disposal containers in Section 6.3 was revised to use the SRNL estimate of tritium release from the disposal containers instead of the PNNL release rate used in the 2008 PA.

Revision 1b November 2021	Section 6.4 was added to describe analysis of vadose zone transport of argon-39 released from TPBAR disposal containers as a special waste form.

EXECUTIVE SUMMARY

In support of the E-Area Performance Assessment, a two-dimensional model of water flow and radionuclide transport through the E-Area Intermediate Level Vault (ILV) and local vadose zone has been developed using the PORFLOW™ software. The purpose of the model is to calculate flux to the water table for radionuclides eluted from the ILV during its operational life, the period of institutional control, and times following site closure. Results of model calculations will be used by a three-dimensional PORFLOW model of transport through the aquifer to determine radionuclide concentrations at a hypothetical 100 meter well and at the site boundary where contaminated groundwater is accessible to members of the public following site closure.

Although newly developed, the model structure closely follows that used in the 2008 PA while incorporating a refined computational mesh, updated material properties for the vadose zone soil and vault concrete, revised infiltration rates, and new solid-liquid distribution coefficients. The model also addresses degradation of concrete hydraulic properties by blending soil and concrete water retention curves over a 500 year period. That is, the hydraulic properties of ILV concrete start out as fresh concrete at the time of site closure and degrade to soil properties over the following 500 years. This approach has not been used previously in E-Area PA's.

The model has been used to calculate water flow through the ILV vadose zone and, on a trial basis, transport of a limited number of radionuclides from the waste region inside the ILV to the water table. Figure ES-1 provides a view of the model and an example of water flow after the concrete has substantially degraded. Figure dimensions are in centimeters. The red area in the left hand side figure is the waste disposal region within the ILV. Colored bands in the figures indicate different soil and concrete regions. Figure ES-2 shows a calculation of flux to the water table (mol/yr) for U-234 and its one-year half-life decay chain (U-234 → Th-230 → Ra-226 → Pb-210). Pb-210 flux is too small to show on the same scale used for Th-230 and Ra-226 in Figure ES-2.

The model has been used to evaluate the release of tritium and argon-39 from TPBAR disposal containers placed in the ILV. Separately calculated tritium and argon-39 release rates as a function of time were used as a source in the PORFLOW model. The TPBAR disposal schedule and tritium release rate differ from the values used in the 2008 PA.

Results from these initial trial runs are compared to calculations made for the 2008 PA ILV analysis. In brief, a new PORFLOW model of flow and transport through the ILV vadose zone has been developed and tested.

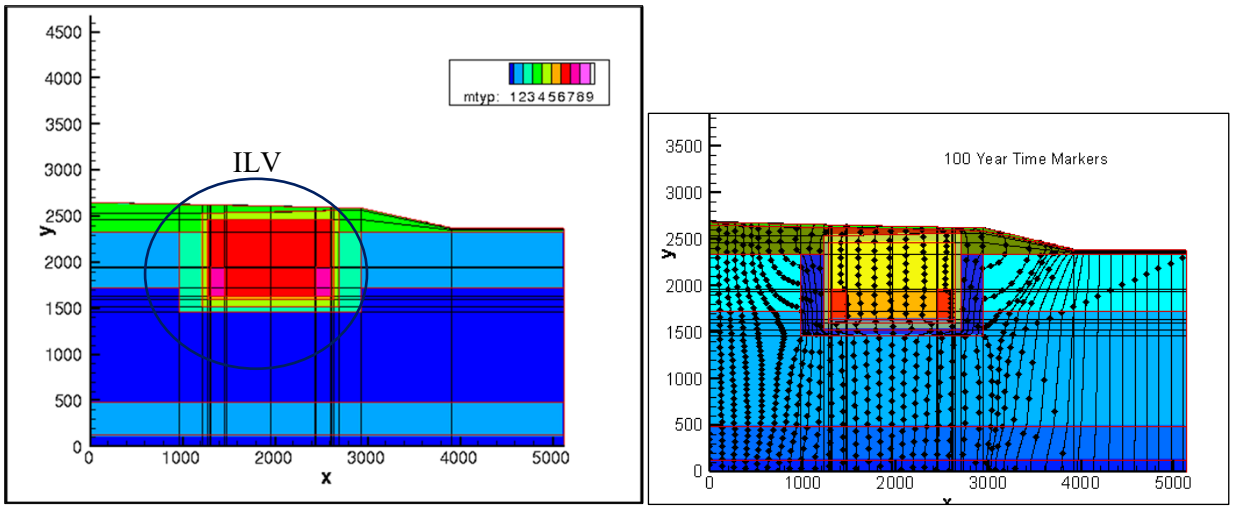

Figure ES-1 ILV Modeling Region and Water Flow 450 to 500 years After Site Closure.

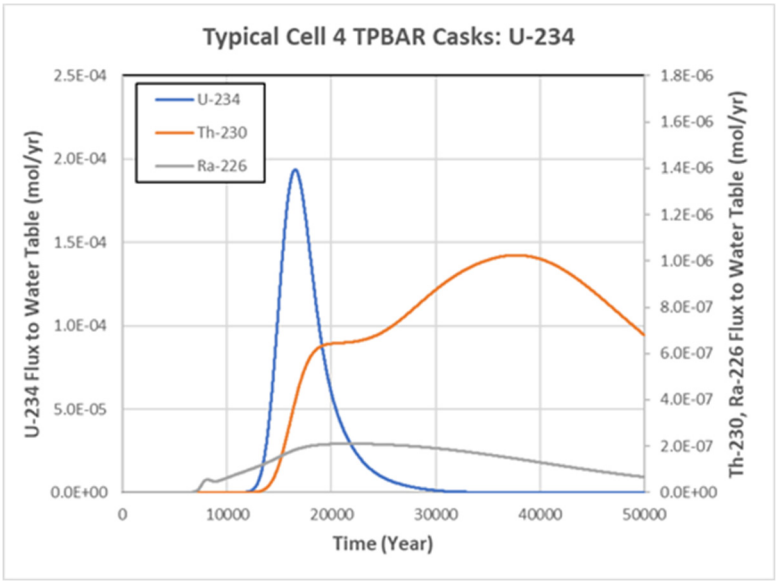

Figure ES-2 Flux to water table for U-234 and daughter radionuclides Th-230 and Ra-226.

TABLE OF CONTENTS

LIST OF TABLES

LIST OF FIGURES

LIST OF ABBREVIATIONS

CLSM	Cementitious Low Strength Material
ELLWF	E-Area Low-Level Waste Facility
GCL	Geosynthetic Clay Layer
GSA	General Separations Areas
HDPE	High Density Polyethylene
HELP	Hydrologic Evaluation of Landfill Performance
IC	Institutional Control
ILNT	Intermediate Level Non-Tritium
ILT	Intermediate Level Tritium
ILV	Intermediate Level Vault
LAZ	Lower Aquifer Zone
LLW	Low Level Waste
LAWV	Low Activity Waste Vault
LVZ	Lower Vadose Zone
OSC	Operational Soil Cover
PA	Performance Assessment
PAWG	Performance Assessment Working Group
PNNL	Pacific Northwest National Laboratory
SA	Special Analysis
SRNL	Savannah River National Laboratory
SRS	Savannah River Site
TCZ	Tan Clay Zone
TPBAR	Tritium Producing Burnable Absorber Rods
UVZ	Upper Vadose Zone
VZ	Vadose Zone
WZ	Waste Zone

1.0 Introduction

The Intermediate Level Vault (ILV) disposal unit is a below-grade reinforced concrete structure containing multiple layers of high-activity waste containers encapsulated by grout or cementitious low strength material (CLSM). The ILV is used to dispose of waste containers exceeding radiological dose and radionuclide concentration limits of other, more cost effective, Low Level Waste (LLW) disposal facilities such as trenches and the Low Activity Waste Vault (LAWV). Figure 1-1 shows the location of the ILV within the E-Area Low Level Waste Facility (ELLWF).

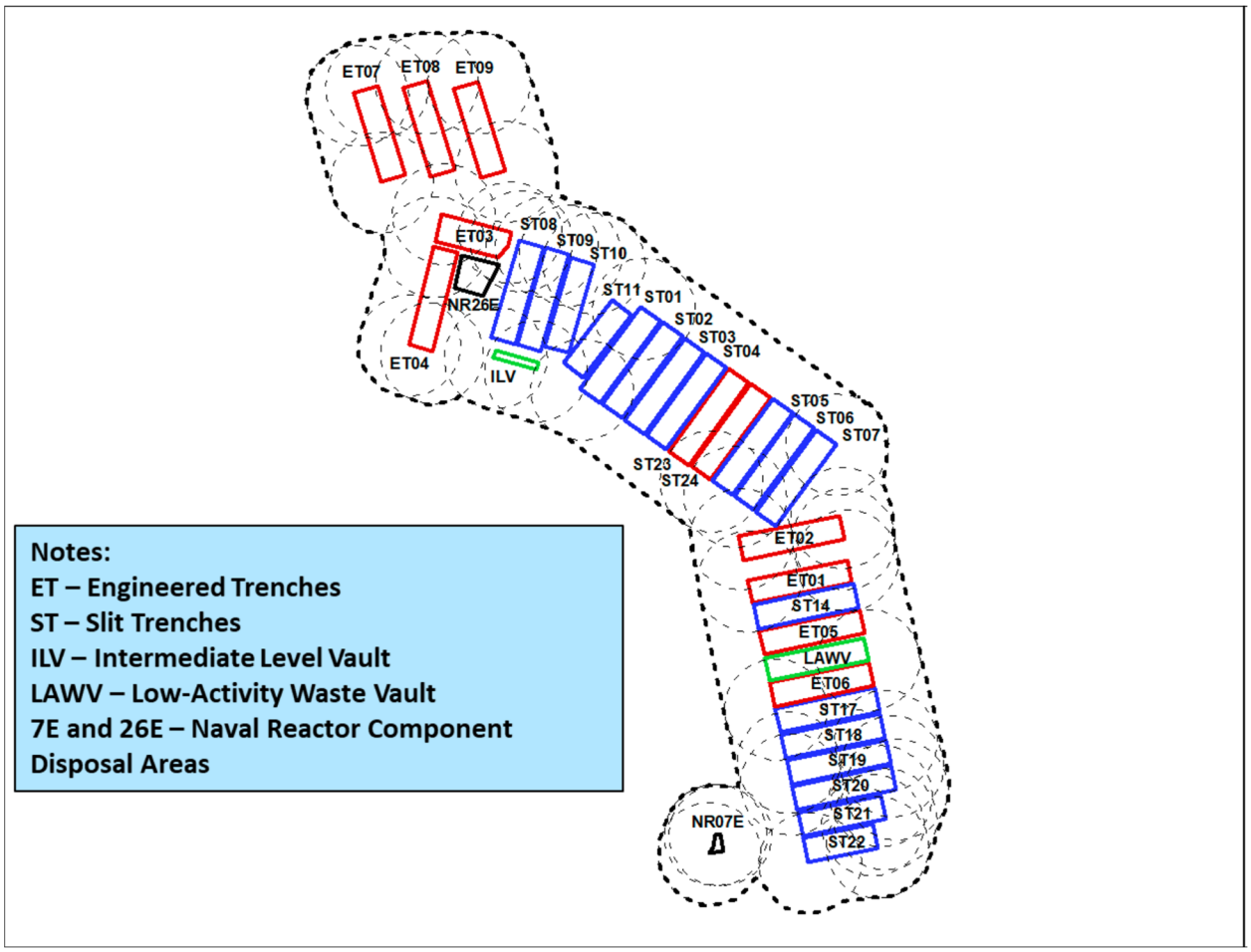

Figure 1-1 Location of Intermediate Level Vault within ELLWF.

2.0 ILV Background

The Intermediate Level Vault is a below-grade, reinforced concrete vault with a total footprint area of 279 feet by 48 feet. The ILV consists of two modules:

1. The Intermediate Level Tritium (ILT) module which contains two cells, whose interior dimensions are 25 feet by 44.5 feet and 26 feet deep.
2. The Intermediate Level Non-Tritium (ILNT) module contains seven cells, whose inside dimensions are 25 feet by 44.5 feet and 28.4 feet deep. The middle or center cell (Cell #4) in the ILNT has slightly different support framing making it more susceptible to cracking under load or during seismic events.

Figure 2-1 shows an aerial view of the ILV exterior with the ILT module in the upper right-hand corner. Figure 2-2 shows an interior view of ILT Cell #2 with some stacked waste containers in place. Figure 2-3 provides a plan view of the operational vault, and Figure 2-4 shows a cross-sectional view of an ILNT cell. The area between the two modules visible in Figures 2-1 and 2-3 provides manhole access to the subdrain system.

ILT Cell #1 contains 144, 20-inch diameter by 20 feet long vertical silos which were originally designed to receive overpacked cylindrical crucibles containing spent reactor targets formerly used in the extraction of tritium for Defense Programs. A total of 35 crucibles were disposed in the ILT Cell #1 silos before a new tritium extraction process became operational resulting in a different spent tritium target waste form. The other 109 silos are currently used for disposing of tritium job control waste and small equipment in 10-gallon drums. The packaged waste is placed in individual silos and a shielding plug is then installed over each silo containing waste.

The remaining eight cells, ILT Cell #2 and ILNT Cells #1 through #7, have open interiors suitable for disposal of large equipment and containers of intermediate-activity waste. As the name implies, the ILNT module was intended to house waste that does not contain significant amounts of tritium. However, ILNT cells have been used for the disposal of steel waste containers containing Tritium Producing Burnable Absorber Rods (TPBAR) which emit tritium by diffusion through the steel and potentially through leaks in welds sealing the waste container lids. During the operational period, intermediate-activity waste is placed in ILT Cell #2 and ILNT Cells #1 through #7 using the following procedure:

- The first layer of waste is placed within each cell directly on top of a graded stone drainage layer.
- When complete, the first layer of waste is encapsulated in grout which forms a surface for the placement of the next layer of waste.
- Subsequent layers of waste are placed directly on top of the previous encapsulated waste; however subsequent layers may be encapsulated with CLSM rather than grout. Figure 2-2 appears to show a second layer of waste being stacked on the grout surface encapsulating the first layer.

Waste placed in ILT Cell #2 and ILNT Cells #1 through #7 typically consists of job control waste, scrap hardware, and contaminated soil and rubble inside metal containers. Containers include drums, B-12 boxes, B-25 boxes, and other metal containers as can be seen in Figure 2-2. Job control waste primarily consists of contaminated protective clothing such as plastic suits, shoe covers, lab

coats, plastic sheeting, and miscellaneous materials. Scrap hardware consists of reactor hardware, jumpers, and used canyon and tank farm equipment. Soil and rubble waste generated from demolition and remediation activities may also be placed in the ILV.

As shown by the photographs and figures below, the ILV has a relatively complicated structure. While some of the other disposal units in the ELLWF will be modeled three-dimensionally in the next PA, it was determined that a two-dimensional model of the ILV cross-section shown in Figure 2-4 would be used. This was the same approach taken in the 2008 PA and is justified by considerations such as:

1. Uniformity of the ILNT cells except for the middle cell which has a construction joint not found in any of the other cells. This makes Cell 4 structurally weaker than other vault cells and subject to greater cracking during seismic events which may require separate modeling.
2. The vault and closure cap are symmetric along the centerline of the short axis.
3. Three-dimensional modeling was used for slit and engineered trenches to capture variations in location relative to the closure cap not seen with the single ILV.

ILV dimensions used to create the PORFLOW™ model were taken from Figure 2-4. Table 2-1 ILV lists significant features of the ILV construction with the modeling approach noted.

.

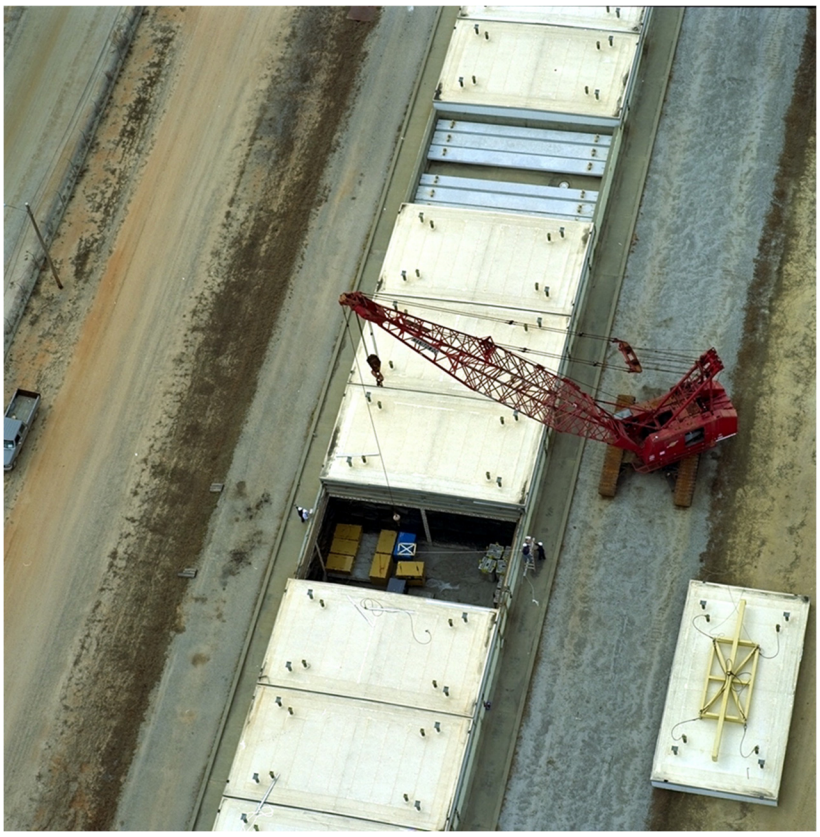

Figure 2-1 Aerial view of ILV.

Figure 2-2 Interior View of ILV Cell.

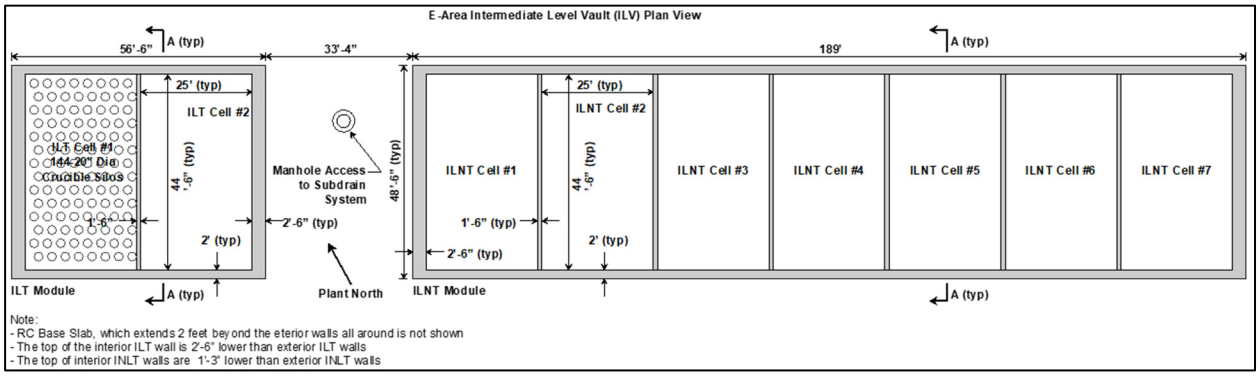

Figure 2-3 Plan view of ILV.

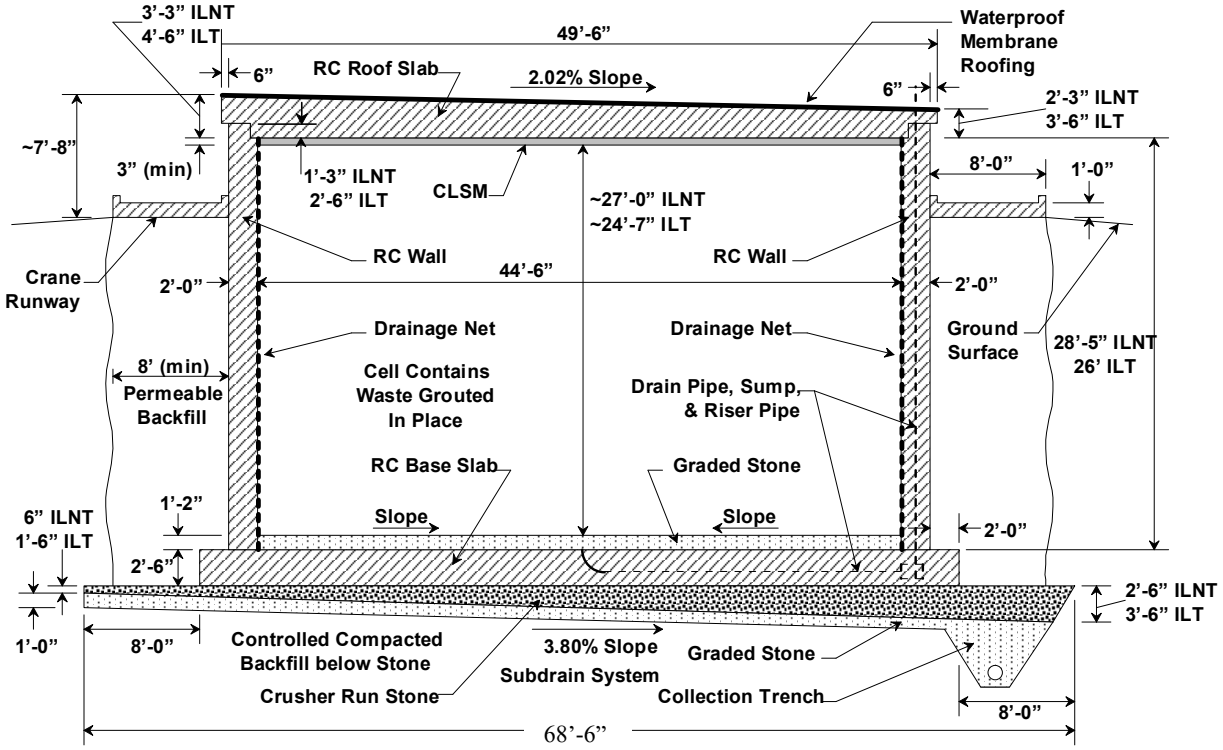

Figure 2-4 Cross-sectional view of ILV.

Table 2-1 ILV Construction Features and Modeling Approach

As Built ILV Features	As Modeled
Controlled compacted backfill soil base	Soil base modeled as ILV backfill.
A graded stone drainage layer with a minimum thickness of 14 inches overlays the floor.	14-inch stone drainage layer above floor modeled as gravel.
Graded stone sub-drainage system to collect and drain any water under the vault to a dry well.	Water under the vault conservatively drains to the water table.
2.5-foot-thick, reinforced concrete, base slab, which extends 2 feet beyond the exterior walls.	2.5-foot concrete base is modeled without the 2-foot extensions beyond wall.
2.5-foot-thick reinforced concrete, exterior end walls, 2-foot-thick reinforced concrete exterior side walls, and 1.5-foot-thick, reinforced concrete interior walls. All walls are structurally mated to the base slab and have no horizontal joints.	Two-dimensional model includes 2-foot side walls.
Sloped rain covers, consisting of a roofing membrane on metal deck on steel framing installed over each cell, to direct rainwater onto the ground for runoff. This is used during operations only and will be replaced with a permanent concrete roof after operations end.	Sloped concrete roof is assumed to be in place throughout the simulation, the metal roof and rain cover would prevent water entering the vault during operations and the model simulates this behavior by using a very low infiltration rate of 0.001 inch/year during ILV operations.
A 3-inch layer of CLSM is used to close filled vault and provide a level surface for roof seating. CLSM or grout is also used to fill and cover waste layers as the vault is filled.	CLSM and grout are modeled indirectly by using radionuclide K_d values for a cementitious environment.

3.0 ILV Timeline

Table 3-1 provides an overview of the ILV timeline assumed in developing the PORFLOW model. The model timing (i.e., Time=0) starts with the receipt of the first disposal container in the ILV in 1995. As a conservative approach, flow and transport modeling assume the entire waste inventory is placed at the start of operations except as discussed for the TPBAR special waste form in Section 6.3. This allows daughter ingrowth to occur for decay chains and does not significantly reduce the concentration of long-lived radionuclides such as C-14, Tc-99 and I-129, which are typically strong contributors to dose. Radionuclides with very short half-lives such as tritium will largely decay away prior to the 1000-year post-closure period during which the performance of the ILV is assessed for regulatory compliance making the assumption of early disposal acceptable.

As described in Section 4.3, hydraulic properties of the vault concrete are assumed to degrade over a 500-year period starting at the end of institutional control when moisture buildup in the overlying cap, vault cracking and lack of access to the subdrain system lead to water infiltration through the vault. Based on a structural analysis performed for the ILV (Peregoy, 2006), installation of the final closure cap results in cracking that partially penetrates the vault walls and roof causing some immediate degradation in concrete hydraulic properties. The structural analysis also concluded that the vault roof would collapse from a seismic event having a 5% probability of occurrence at a mean time of 6250 years. As explained in the discussion of infiltration rates in Section 4.2, the time of roof collapse was assumed to be 5770 years in the model to coincide with an existing infiltration rate calculation.

Table 3-1 ILV Timeline

Calendar Date	Numerical Calendar Date	Time from Start of ILV Operation	Operational Events
9/28/1994	1994.74	-1.0	Start of ELLWF operations.
9/28/1995	1995.74	0.0	Start of ILV operations.[1,2] Start radionuclide decay and daughter ingrowth. Start 10,000-year modeling period.
9/28/2040	2040.74	45.0	ILV filled ending operations. Metal roof replaced with final concrete roof having a rain cover.
9/28/2065	2065.74	70.0	End of ELLWF operations. Start of institutional control.
9/28/2165	2165.74	170.0	End of institutional control. Installation of final closure cap. Non-through cracking of vault roof and walls. End of water removal from vault sump. Start 500-year concrete degradation. Start 1000-year compliance period.
9/28/2665	2665.74	670.0	Vault concrete fails hydraulically.
9/28/3165	3165.74	1170.0	End of 1000-year compliance period.
9/28/7775	7775.74	5770.0	Vault roof collapses. Waste material subsides into 10 ft layer at bottom of vault.
9/28/12165	12165.74	10170.0	End of 10,000-year modeling period.[3]

[1]Conservativly, it is assumed that all the waste in the ILV (exclusive of TPBAR waste containers) is placed at the start of operation. TPBAR waste container disposal in the model follows the waste management disposal schedule.
[2]The earliest recorded date for disposal in the ILV is 5/12/1995. This information was found after the model was developed and the difference in using 9/28/1995 deemed to be within modeling uncertainty.
[3]For some radionuclides, modeling will be extended to 50,000 years to capture peak radionuclide concentrations.

4.0 ILV Vadose Zone Hydro-stratigraphic Layers

Figure 4-1 shows a generalized (not to scale) one-dimensional schematic diagram of the ILV disposal site and the underlying vadose zone hydro-stratigraphic layers. The diagram is only intended to show the vadose zone layers and omits many details of the actual PORFLOW model. Dimensions of the zones for the ILV disposal site (Bagwell and Bennett, 2017) and specification of soil material in the model are listed in Table 4-1. The PORFLOW model used in the 2008 PA did not include the Tan Clay or Lower Aquifer zones.

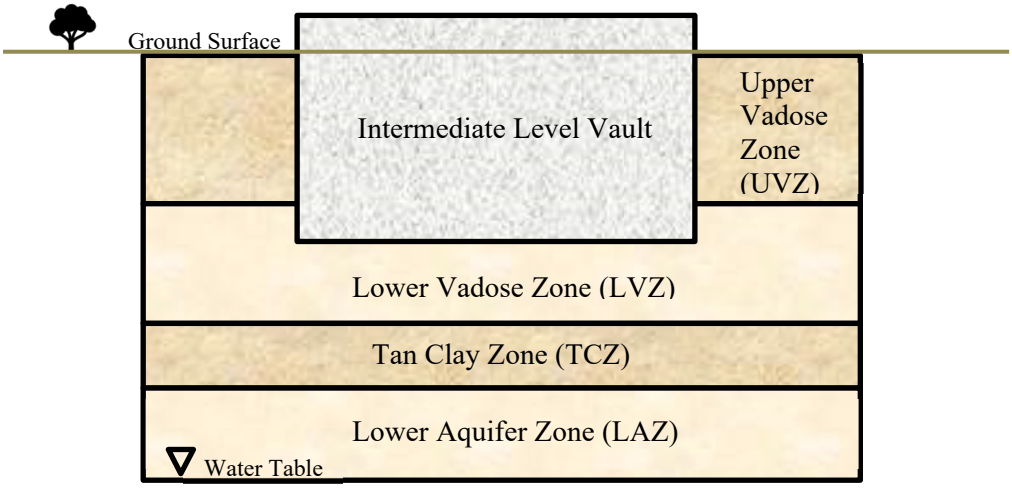

Figure 4-1 Schematic representation of ILV waste disposal site and vadose zone hydro-stratigraphic layers.

Table 4-1 Nominal Thickness in Feet and Composition of ILV Vadose Zone Segments

Vadose Zone Segments	Segment Length (feet)
Average Depth to Water Table	76.5 feet
UVZ	19.9 feet Clay
LVZ	40.8 feet Sand
TCZ	11.7 feet Clay
LAZ	4.1 feet Sand

5.0 Model Description

5.1 ILV Model Geometry

Figure 5-1 provides a cross-sectional view of the ILV with the final closure cap in place taken from design document C-CT-E-00084. The ILV site is located along the southern perimeter of the ELLWF area. Therefore, as shown in Figure 5-1, the final closure cap will slope down to ground level 40 feet south of the ILV. As discussed below in Section 5.2, infiltration rates calculated to pass through the High-Density Polyethylene (HDPE) geomembrane which lies just above the Geosynthetic Clay Layer (GCL) are used as an upper boundary condition in the PORFLOW model. The geomembrane is the limiting barrier to infiltration in the closure cap design. The PORFLOW model includes a structural soil layer placed over the vault (referred to as the "foundation layer" in Figure 5-1) forming the slope and supporting the overlying closure cap. Infiltration through the geomembrane reaches the top surface of this soil layer which then forms the upper boundary of the model.

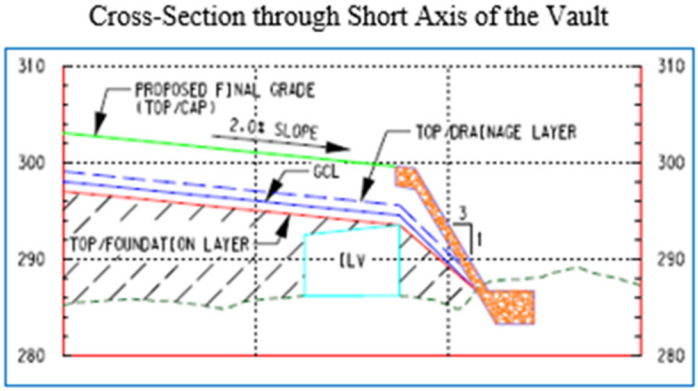

Figure 5-1 Detail of ILV Final Closure Cap Configuration (C-CT-E-00084, 2016).

Three two-dimensional models perpendicular to the long axis of the ILV facility were developed:

1. A model of the center ILNT cell (Cell #4) containing no TPBAR waste containers shown in Figure 5-2. The red region in the center of the vault is the region where waste material is disposed.
2. A model of a typical ILNT cell containing four TPBAR waste containers shown in Figure 5-3. The four TPBAR waste containers are in two stacks with two waste containers in each stack located one foot from the vault walls. Each stack is assumed to be 10 feet high.
3. A model of a typical ILNT cell containing eight TPBAR waste containers shown in Figure 5-4. The eight TPBAR waste containers are in four stacks with two waste containers in each stack located one foot from the vault walls.

In Figure 5-2 through Figure 5-4 horizontal and vertical dimensions are in centimeters. Therefore, the 5136 cm horizontal dimension represents a model domain 168.5 feet in length. The vault is 48.5 feet (1478 cm) wide with the computational grid extending 40 feet (1219 cm) to the left of the vault (upslope – northern side of the closure cap) and 80 feet (2438 cm) to the right (downslope - southern side). The additional 40 feet further south includes an area not under the closure cap to account for possible flow into the vadose zone beneath the ILV from background infiltration. The

ILV roof slopes about 2% from south to north while the closure cap slopes about 2% in the opposite direction. The model includes these sloped surfaces and, as can be seen by comparison with Figure 5-1, the model captures the closure cap slope to ground level south of the ILV.

Figure 5-5 shows a close-in view of the computational mesh immediately around the ILV. This figure gives an indication of the mesh detail and provides a better view of the vault concrete and the surrounding soil. The same basic computational mesh was used for the three modeling cases with different mesh structure around TPBAR disposal containers and tritium release zones for each case.

The ILV was constructed on a controlled compacted soil base in an excavated region of the vadose zone to provide a foundation for the vault floor and sub-floor drainage system. Controlled compacted soil was then added as fill around the vault walls to ground surface for support of the vault walls and gantry crane runway along the sides of the vault. (Use of a gantry crane for waste disposal operations was ultimately abandoned in favor of a stick crane – see Figure 2-1). At final closure, controlled compacted soil will be built up across the entire ELLWF footprint as a foundation layer for the closure cap. As stated earlier, this foundation layer of the closure cap above and adjacent to the ILV serves as the top boundary of the PORFLOW model where infiltration is applied. The model assumes that the crane runway will be removed at site closure.

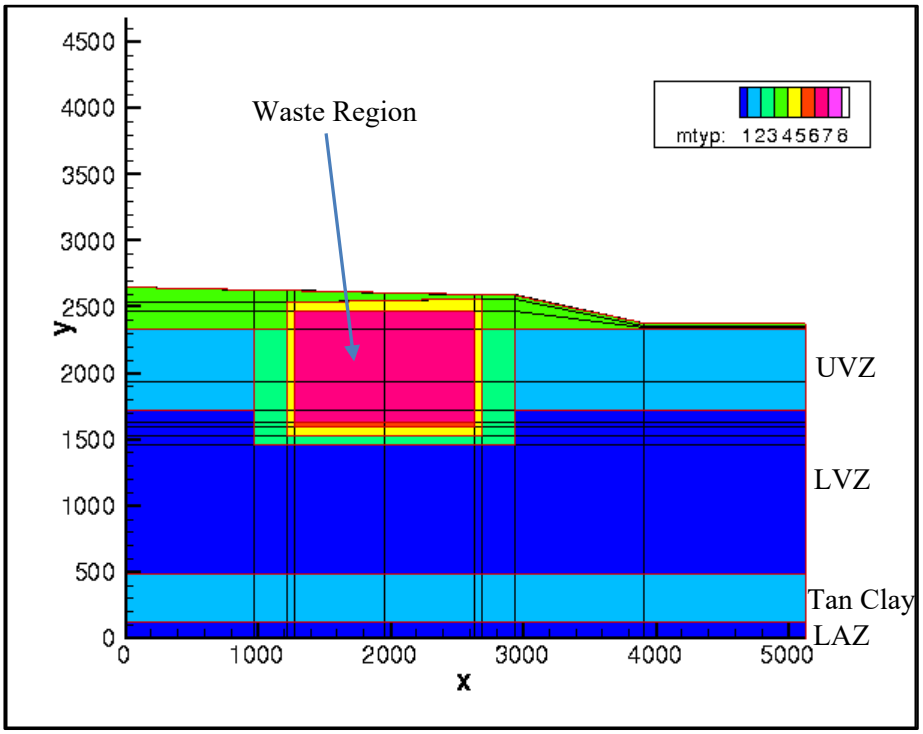

Figure 5-2 Model of Center ILNT cell having no TPBAR waste containers.

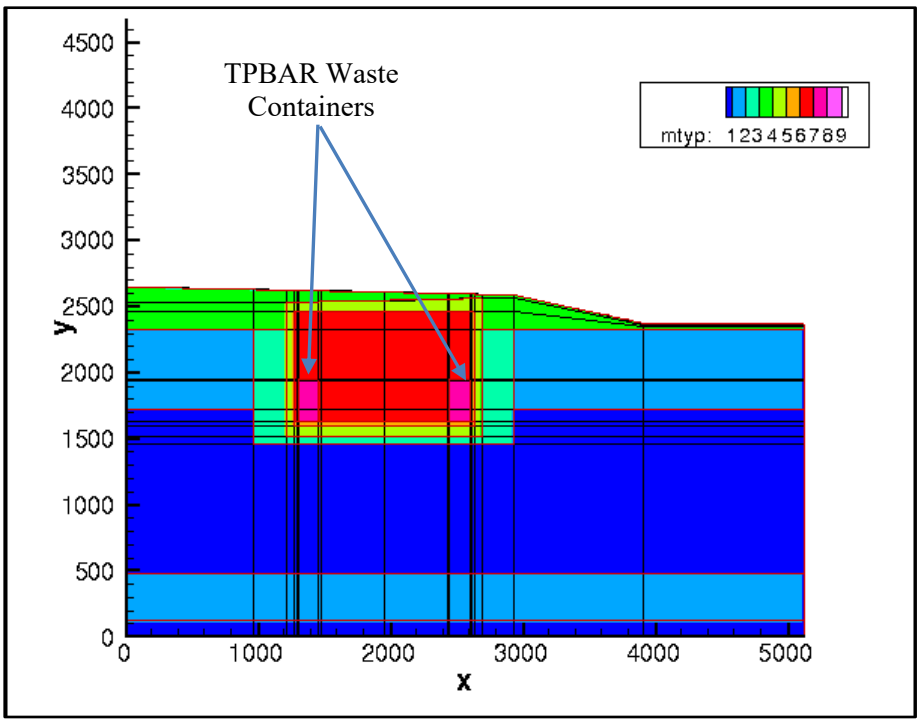

Figure 5-3 Model of Typical ILNT cell with 4 TPBAR waste containers in 2 stacks of 2.

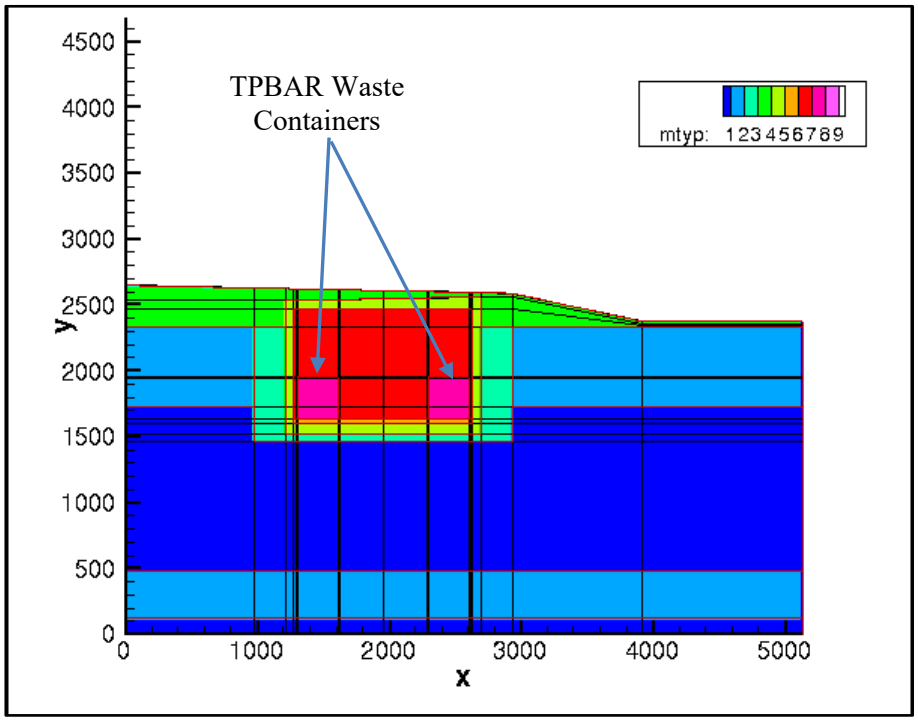

Figure 5-4 Model of Typical ILNT cell with 8 TPBAR waste containers in 4 stacks of 2.

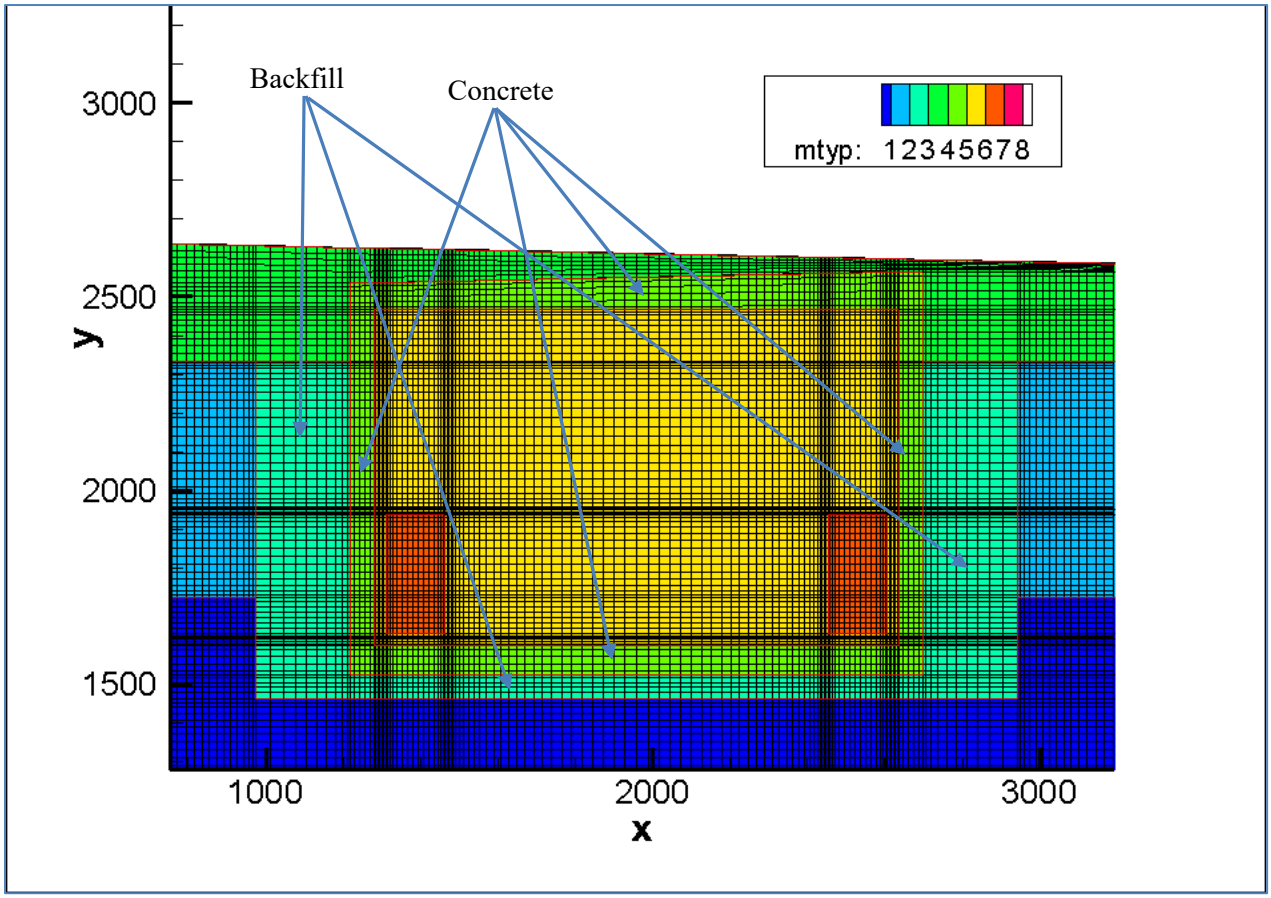

Figure 5-5 Computational Mesh Around Vault in Model of Typical ILNT cell.

5.2 Infiltration Boundary Conditions

Infiltration rates through the ILV and surrounding area used in the PORFLOW model are listed in Table 5-1. During operations, the vault has a removable metal roof allowing access to the cells for waste disposal as can be seen in Figure 2-1. The metal roof prevents rainwater from entering the waste cells. It is assumed that the ILV will be filled by the year 2040 at which time the metal roof will be replaced with a permanent sloped reinforced concrete roof slab with overlying bonded-in-place fiberboard insulation and a waterproof membrane (Dyer, 2019). For modeling purposes, the permanent concrete roof is assumed to be in place throughout the ILV operating period and the function of the metal roof and rain cover are modeled by applying a very low infiltration rate (0.001 in/yr) during this time.

This sloped permanent reinforced concrete roof with overlying waterproof membrane will remain uncovered during the remaining E-Area operational period (2040-2065) and the following 100-years of institutional control (2065-2165). There will essentially be no water infiltration into the vault during this time for the following reasons:

- A 2% roof slope and overlying waterproof membrane shed rainwater from the top of the vault

- The initial intact condition of the ILV roof will be maintained during the remaining E-Area operations after the ILV is closed and the following institutional control period.
- Absence of a soil cover during this period prevents buildup of soil moisture above the roof.

Thus, for modeling purposes, a small infiltration of 0.001 in/yr is assumed to apply for the first 170 years of the simulation.

At the end of institutional control, a final soil-geomembrane closure cap will be placed over the entire ELLWF. Infiltration rates above the ILV and the surrounding soil cover from the time of final closure cap placement to 7100 years, when it was assumed that the vault roof would collapse, have been calculated using the Hydrologic Evaluation of Landfill Performance (HELP) model (Dyer, 2019). Beyond 7100 years infiltration rates are assumed to remain constant. An ILV structural analysis (Peregoy, 2006) determined the mean time to roof collapse from a seismic event to be 6250 years. To be slightly conservative and to avoid revising the HELP calculations, the PORFLOW model assumed ILV roof collapse occurs at 5770 years where a HELP infiltration rate had already been calculated. That is, infiltration rates through the closure cap over the ILV calculated using the HELP model were used for the first 5770 years of modeling. At 5770 years, the constant infiltration following roof collapse calculated with the HELP was applied.

During the 500 years following the end of institutional control, the model degrades concrete hydraulic properties and at 500 years assumes that hydraulically the concrete behaves like soil. The model adjusts concrete properties in 50-year time steps by blending hydraulic properties for concrete with those of operational soil cover. Because these steps did not coincide with the HELP model infiltration calculations the HELP results were linearly interpolated to follow the 50-year incremental changes in material properties. Subsequently, it was decided to further refine the flow solution by adding more time steps interpolated from the HELP calculations. The results of this interpolation are shown in Table 5-1. The shaded area from 170 to 670 years is the time when concrete degradation occurs. Flows in the table are shown as follows:

1. Infiltration from time 0 to 170 years is 0.00010 inch/yr.
2. At 170 years the infiltration changes to 0.00015 inch/yr.
3. Thereafter, infiltration values at the beginning of the indicated time period are shown. For example, infiltration changes from 0.00015 inch/year to 0.00062 inch/yr at 220 years.
4. PORFLOW input processing takes the average of the starting and ending infiltrations as the steady-state flow for the time period.

Table 5-1 also shows that, after the final closure cap is in place, infiltration over the vault ("on-vault" infiltration) and the 40-foot capped regions on either side of the vault ("off-vault" infiltration), are identical until the vault roof collapses at 5770 years. Following roof collapse, flow through the vault is greater than the background value because the gap in the closure cap collects runoff from the upslope portion of the intact cap. Infiltration in areas not under the closure cap have an assumed background value of 15.78 inch/yr (40 cm/yr).

A detailed description of the method used to calculate hydraulic properties for concrete mixed with soil is contained in Section 5.3.

Table 5-1 ILV Infiltration Rates: HELP Infiltration with Closure Cap Intact Until 5770 Years

	Numerical Calendar Date	Time from Start of ILV Operation	ILV Event	On-Vault Infiltration (inch/year)	Off-Vault[1] Infiltration (inch/year)
1	1995.74	0.0	Start of ILV Operations	0.00010	15.78
	2040.74	45.0	ILV Closed		
	2065.74	70.0	Start of IC[2]		
	2165.74	170.0	End of IC Closure Cap Installed Start of Compliance Period	0.00015	0.00015
2	500 Year Period of Concrete Degradation	220.0		0.00062	0.00062
3		270.0		0.00437	0.00437
4		320.0		0.01305	0.01305
5		370.0		0.022	0.022
6		420.0		0.085	0.085
7		470.0		0.162	0.162
8		520.0		0.317	0.317
9		570.0		0.496	0.496
10		620.0		0.709	0.709
11		670.0	Vault Hydraulic Failure[3]	0.923	0.923
12	2725.74	720.0		1.137	1.137
13		770.0		1.424	1.424
14		820.0		1.728	1.728
15		870.0		2.033	2.033
16		920.0		2.337	2.337
17		970.0		2.642	2.642
18		1020.0		2.946	2.946
19		1070.0		3.251	3.251
20		1120.0		3.555	3.555
21	3165.74	1170.0	End of Compliance Period	3.860	3.860
22		1320.0		4.764	4.764
23		1470.0		5.668	5.668
24		1620.0		6.571	6.571
25		1770.0		7.475	7.475
26		1920.0		8.379	8.379
27		2070.0		8.913	8.913
28		2220.0		9.263	9.263
29		2370.0		9.613	9.613
30		2520.0		9.963	9.963
31		2670.0		10.313	10.313
32		2820.0		10.606	10.606
33		3370.0		10.710	10.710
34		5770.0		10.890	10.890
35		5770.1	Vault Roof Collapse, Closure Cap Over ILV Fails	36.85[4]	10.94
	12,165.74	50,000	End of Simulation	36.85	10.94

[1]Infiltration on either side of vault
[2]Institutional Control
[3]Vault concrete fails hydraulically, closure cap remains intact
[4]Following vault roof collapse, flow through the ILV increases due to closure cap runoff

5.3 Modeling of Concrete Degradation

In past PA's, the hydraulic properties of concrete have been abruptly changed from those of intact concrete to soil to represent vault structural collapse or complete deterioration of the concrete matrix. For this PA, concrete degradation is modeled as a gradual process where, starting at the time of site closure, concrete hydraulic properties are adjusted to those of soil over a period of 500 years. The 500-year post closure end point is adopted from the PA Working Group (PAWG) recommendation in NUREG-1573. An excerpt from this document (¶2 Section 3.2 "Performance of Engineered Barriers") is reproduced below:

> However, to limit unnecessary speculation as to their performance, the PAWG believes that materials typically used in engineered barriers can alternatively be assumed to have physically degraded after 500 years following site closure. Thus, at 500 years and beyond, the engineered barriers can be assumed to function at levels of performance that are considerably less than their optimum level, but credit for structural stability and chemical buffering effects may be taken for longer periods of time.[1] For timeframes longer than 500 years, it is unreasonable to assume that any physical engineered barrier such as a cover or a reinforced concrete vault can be designed to function long enough to influence the eventual release of long-lived radionuclides such as carbon-14 (half-life: 5300 years); technetium-99 (half-life: 213,000 years); and iodine-129 (half-life: 15,700,000 years), if they are present. However, credit for structural stability and chemical buffering effects may be taken for the long-term provided that the applicant provides suitable information and justification. But again, this would have to be evaluated on a case-by-case basis.

Based on this recommendation, the ILV model uses a blend of concrete and soil to determine hydraulic properties in 50-year increments over the assumed 500-year lifetime of the ILV concrete. At site closure, structural analysis of the ILV (Peregoy, 2006) predicts that the ILV roof and walls will experience limited non-through static cracking upon application of the final closure cap over the vault. Upon final closure, initial hydraulic properties for vault roof and wall concrete are taken to be a blend of 90% E-Area Vault Concrete and 10% Gravel to represent the impact of early stress cracking in the concrete. Soil blended with the concrete is represented by the hydraulic properties of operational soil cover before dynamic compaction (OSC1) (Nichols and Butcher, 2020). Table 5-2 provides a list of the material blends used to represent concrete degradation following site closure.

Table 5-2 Material Blends for Degraded Concrete

Years Post Closure	ILV Roof and Walls		ILV Floor	
	90% Concrete 10% Gravel	Soil	E-Area Concrete	Soil
0	100%	0%	100%	0%
50	90%	10%	90%	10%
100	80%	20%	80%	20%
150	70%	30%	70%	30%
200	60%	40%	60%	40%
250	50%	50%	50%	50%
300	40%	60%	40%	60%
350	30%	70%	30%	70%
400	20%	80%	20%	80%
450	10%	90%	10%	90%
500	0%	100%	0%	100%

5.3.1 Property Blending

Hydraulic properties for a mixture of concrete and another material (in this case soil) are typically calculated as described by Flach (2017). Composite porosity (ϵ_b) and saturated hydraulic conductivity (K_b) are calculated from the equations:

$$\epsilon_b{}^p = f_c\,\epsilon_c{}^p + f_s\,\epsilon_s{}^p \quad (1)$$

$$K_b{}^p = f_c\,K_c{}^p + f_s\,K_s{}^p \quad (2)$$

where:

ϵ ..... porosity
K ..... saturated hydraulic conductivity
f_c ..... volume fraction concrete
f_s ..... volume fraction soil = $(1 - f_c)$
p ..... factor used to choose either:
arithmetic ($p = 1$),
geometric ($p \to 0$), or
harmonic ($p = -1$) blending
b ..... blend
c ..... concrete
s ..... soil

Saturation and hydraulic conductivity for a composite material as functions of suction pressure (ψ) are calculated from the equations:

$$[\epsilon_b\,S(\psi)_b]^p = f_c\,[\epsilon_c\,S(\psi)_c]^p + f_s\,[\epsilon_s\,S(\psi)_s]^p \quad (3)$$

$$[K_b\,k_h(\psi)_b]^p = f_c\,[K_c\,k_h(\psi)_c]^p + f_s\,[K_s\,k_h(\psi)_s]^p \quad (4)$$

where:

$k_h(\psi)$ ..... hydraulic conductivity as a function of suction pressure
$S(\psi)$ ..... saturation as a function of suction pressure
ψ ..... suction pressure

Example results for hydraulic conductivity obtained by blending E-Area Vault Concrete with OSC1 using arithmetical averaging are shown in Figure 5-6. Using this blending method, a small amount of soil significantly alters the hydraulic conductivity. This occurs because the method is making a homogeneous blend and a small amount of soil can lead to a large increase in water flow through a homogeneously mixed material. That is, the material with the largest conductivity is weighted the most. Using the harmonic blending method gives the results shown in Figure 5-7. In this case, the concrete properties are more heavily weighted. That is, the material with the smallest conductivity is weighted the most. Years in both figure legends correspond with the concrete-soil blends in Table 5-2.

Since neither of the blending methods shown in Figure 5-6 and Figure 5-7 appeared to represent concrete degradation satisfactorily, geometric averaging was employed using Eqns. (3) and (4) with a small value of the factor p ($p = 0.01$). Results obtained using this blending method are shown in Figure 5-8 and Figure 5-9. These results appeared to show a reasonable blending to represent the change in concrete properties over time and were adopted for use in the ILV model.

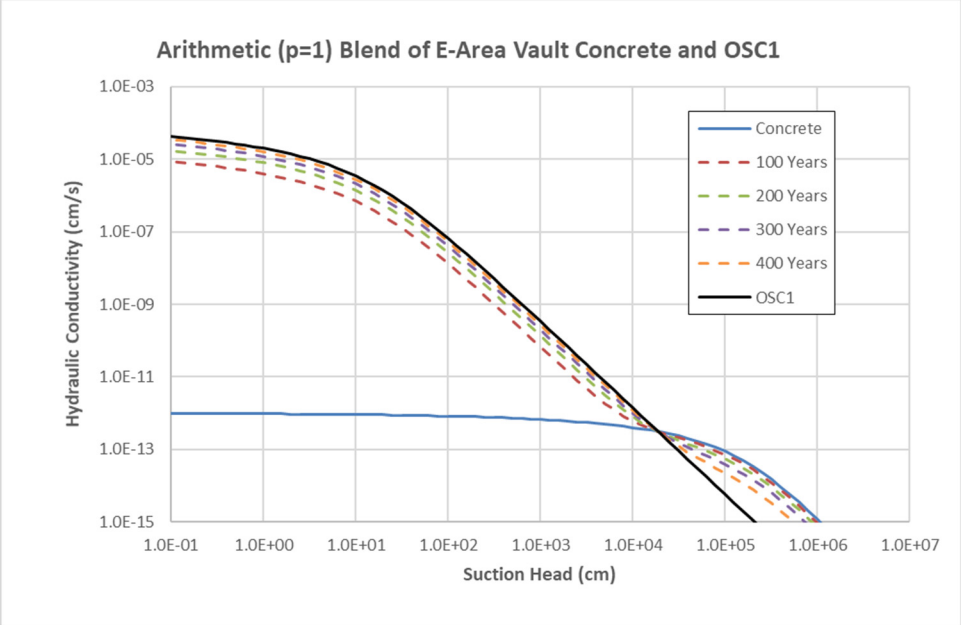

Figure 5-6 Hydraulic conductivity for blends of E-Area vault concrete and OSC1 calculated using arithmetical averaging method.

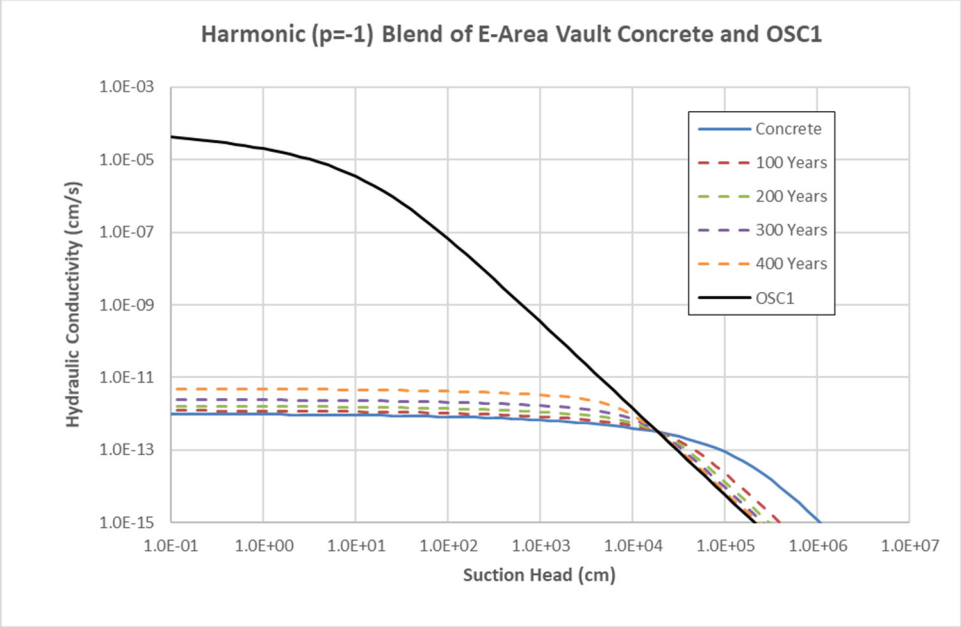

Figure 5-7 Hydraulic conductivity for blends of E-Area vault concrete and OSC1 calculated using harmonic averaging method.

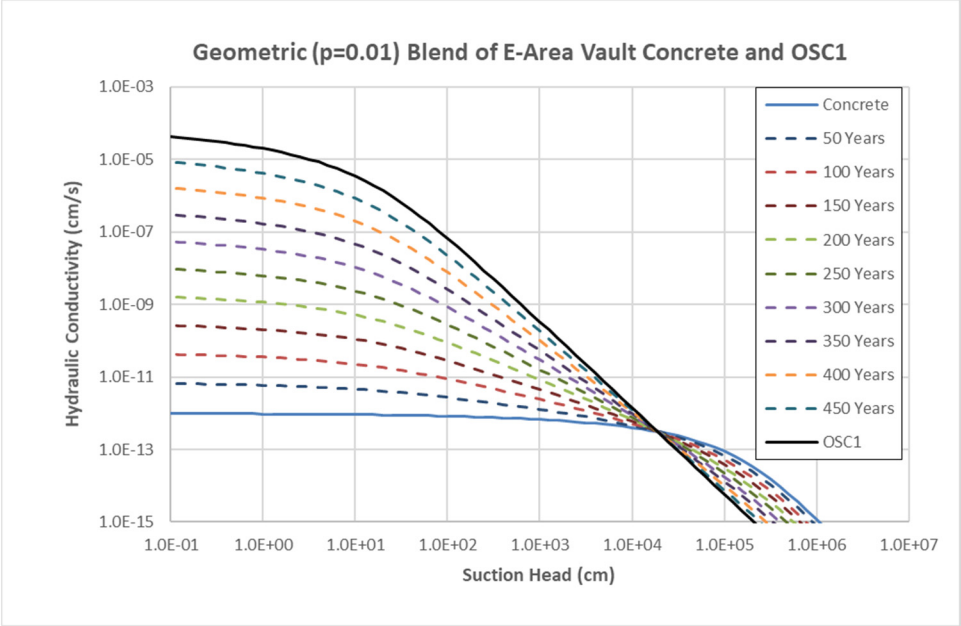

Figure 5-8 Hydraulic conductivity for blends of E-Area vault concrete and OSC1 calculated using geometric averaging method.

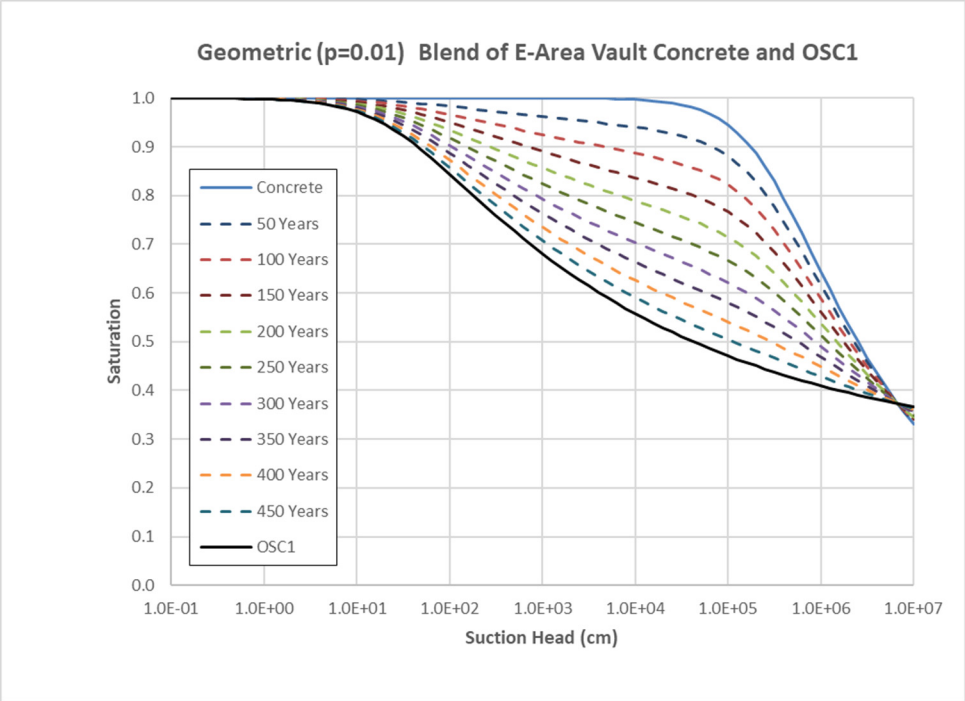

Figure 5-9 Water saturation for blends of E-Area vault concrete and OSC1 calculated using geometric averaging method.

6.0 Model Results

6.1 Vadose Zone Flow

PORFLOW modeling is used to calculate a steady-state flow field for each of the 35 time intervals listed in Table 5-1. Results obtained include the infiltration water flow, water saturation in materials, and suction pressure throughout the three computational domains shown in Figure 5-2 through Figure 5-4. In addition, information on the deviation of saturation from the water retention curves and convergence of the flow calculations can be obtained. To simplify the data presented in this report, the ILV model having four TPBAR waste containers (Figure 5-3) was chosen as the nominal case. To simplify figure captions, the terminology "waste containers" is omitted and "4 TPBAR ILV model" used to identify the case. Flow patterns obtained with the other two PORFLOW models were very similar to those shown below. Results for the steady-state flow fields are presented in this section of the report and results for saturation and pressure are consigned to Appendices A and B, respectively. Diagrams of steady-state flow based on the Darcy velocity during each simulation time period are shown in Figure 6-1 through Figure 6-9. Corresponding infiltration flows are listed in Table 5-1. Showing results for all 35 time periods was considered excessive so only the 18 results at odd number time intervals are shown.

Figure 6-1 shows the flow field from the start of ILV operations until the end of institutional control and 50 to 100 years following closure cap installation. As shown in Figure 2-1, during ILV operations, a temporary metal roof with a rain cover is in place over each cell to allow access for waste disposal. At the end of operations, the metal covers will be removed and replaced with a permanent concrete

roof covered by a waterproof membrane. During these early time periods, it is assumed that the metal rain covers over each cell and the waterproof membrane covering the concrete roof are actively maintained and infiltration into the vault is nearly zero (0.001 in/yr). As described in Section 5.1, the PORFLOW two dimensional model domain extends 40 feet north (upslope) of the vault and 80 feet south of the vault (the south side includes 40 feet from the ILV wall to the edge of the cap plus an additional 40 feet of uncovered soil beyond the edge). Figure 6-1 shows that before the closure cap is placed (Figure 6-1 left), flow through the vault is essentially zero and some of the water infiltration beside the vault is diverted underneath the ILV. After the closure cap is placed in year 170, Figure 6-1 (right) shows that infiltration through the fresh cap is very small but some flow from the uncovered region to the right of the ILV encroaches below the vault.

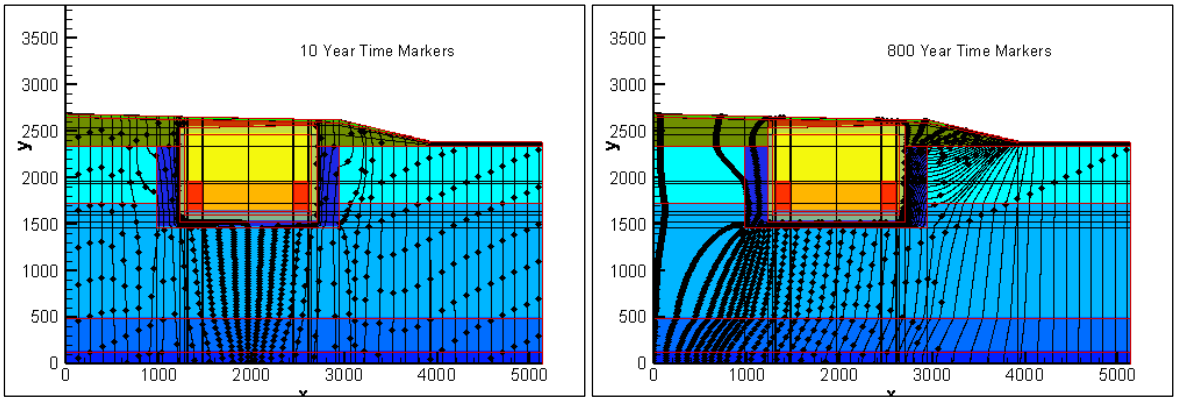

Figure 6-1 Flow field in 4 TPBAR ILV model: (0 – 170) years and (220 – 270) years.

The hydraulic performance of both the closure cap and the vault concrete begin to deteriorate starting at 170 years. The predicted flow fields from 150 to 200 years and 250 to 300 years following site closure are shown in Figure 6-2. During this time, the closure cap performs well, the concrete is relatively intact and infiltration through the vault itself remains low. Time markers in Figure 6-2 are placed at 300-year and 100-year intervals. Therefore, while the figures show channeling of water to the sides and below the vault, the actual flow near the vault is small.

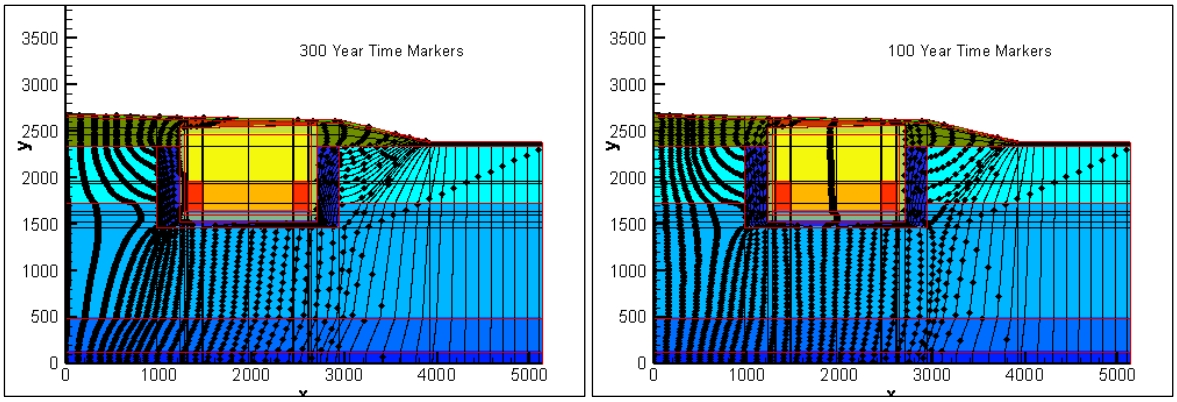

Figure 6-2 Flow field in 4 TPBAR ILV model: (320 – 370) and (420 – 470) years.

Figure 6-3 shows water infiltration from 350 to 400 and from 450 to 500 years after closure cap installation. The 500-year period from 170 years to 670 years is the time during which degradation of the vault concrete is modeled as described in Section 5.3. Progressive deterioration in the hydraulic behavior of both the closure cap and vault concrete over this time is evident in this set of figures. In fact, comparison with Figure 6-1 shows a significant change with noticeable flow through the ILV. However, as the 100 and 50 year time markers indicate, the flow rate is still relatively small. The vault concrete is assumed to completely fail hydraulically at 670 years when it takes on the hydraulic properties of OSC1 (clayey soil). From this point on, further increases in the infiltration through the vault are caused by deterioration of the geomembrane layer in the closure cap.

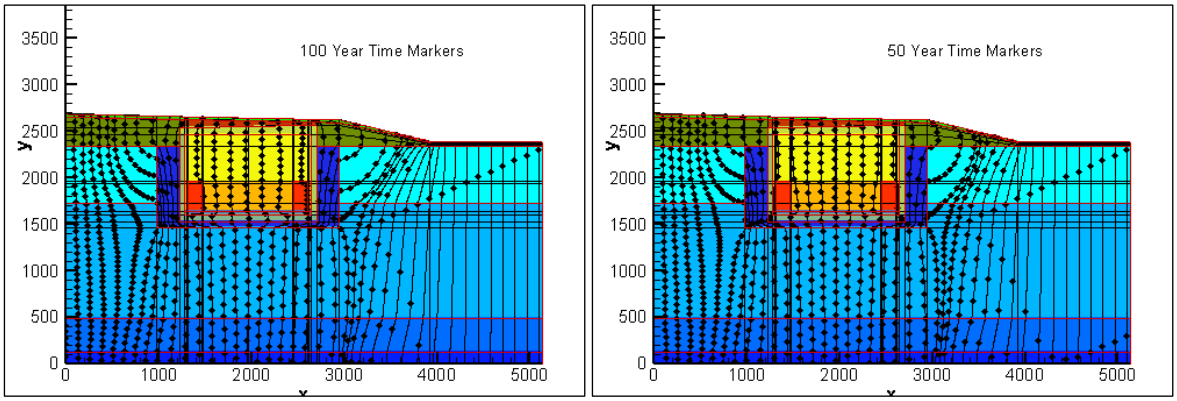

Figure 6-3 Flow field in 4 TPBAR ILV model: (520 – 570) and (620 – 670) years.

Figure 6-4 through Figure 6-6 show infiltration flow fields from 720 years to 1470 years. Progressive deterioration in the hydraulic behavior of the closure cap over this time is evident in this set of figures. Note that the spacing between time markers decreases from 40 years to 20 years in this sequence indicating increased flow rates. It is notable that flow through the ILV becomes very uniform following concrete degradation. It should also be noted that in this and the other flow figures there is no flow through the TPBAR disposal containers as was intended. The 1000 year period of compliance ends at 1170 years so results beyond this set of figures will have no impact on disposal limits.

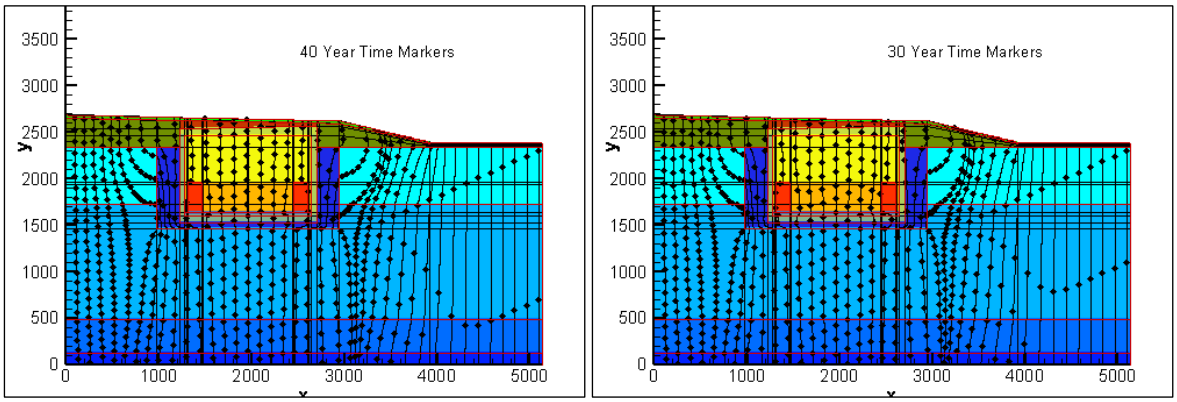

Figure 6-4 Flow field in 4 TPBAR ILV model: (720 – 770) and (820 – 870) years.

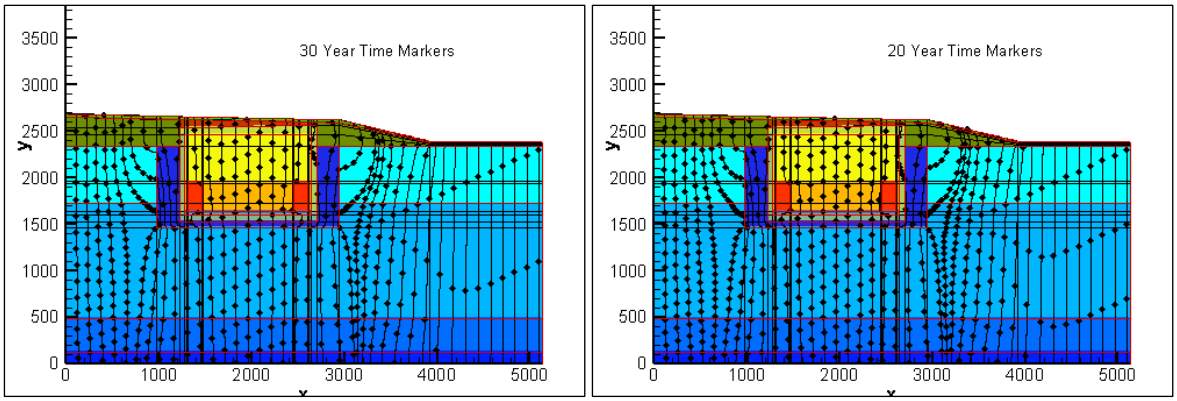

Figure 6-5 Flow field in 4 TPBAR ILV model: (920 – 970) and (1020 – 1070) years.

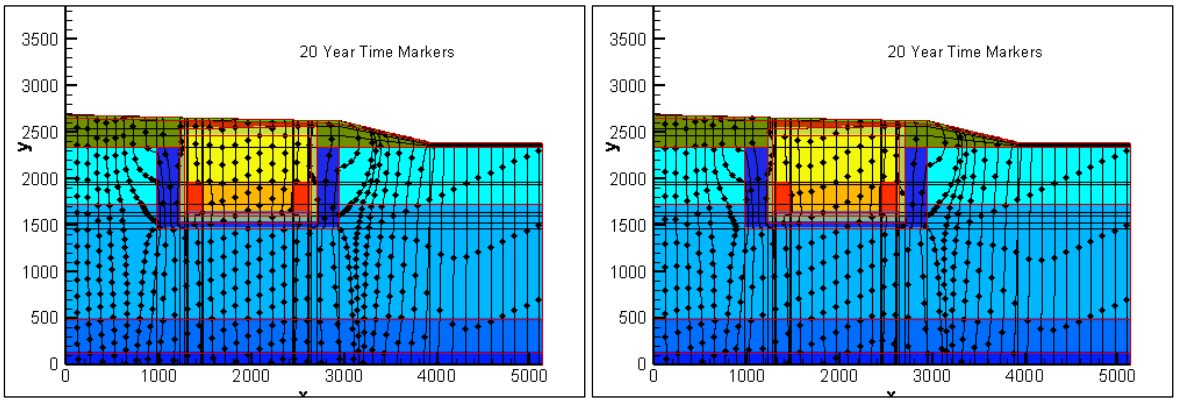

Figure 6-6 Flow field in 4 TPBAR ILV model: (1120 – 1170) and (1320 – 1470) years.

Figure 6-7 through Figure 6-9 show flow during years beyond the compliance period. The flow increases as degradation of the geomembrane continues. After 1770 years, flow has increased enough such that 10-year markers are used to better illustrate the flow pattern. As shown in Table 5-1, between 1970 and 5770 years the infiltration flow does not change significantly.

At 5770 years the vault roof is assumed to collapse increasing flow through the vault region as runoff from the upslope intact closure cap enters the space created by roof collapse. Beyond 5770 years, this flow pattern is assumed to remain unchanged. The final ILV vadose zone flow is shown in the right hand side of Figure 6-9 where high flow through the vault area is evident.

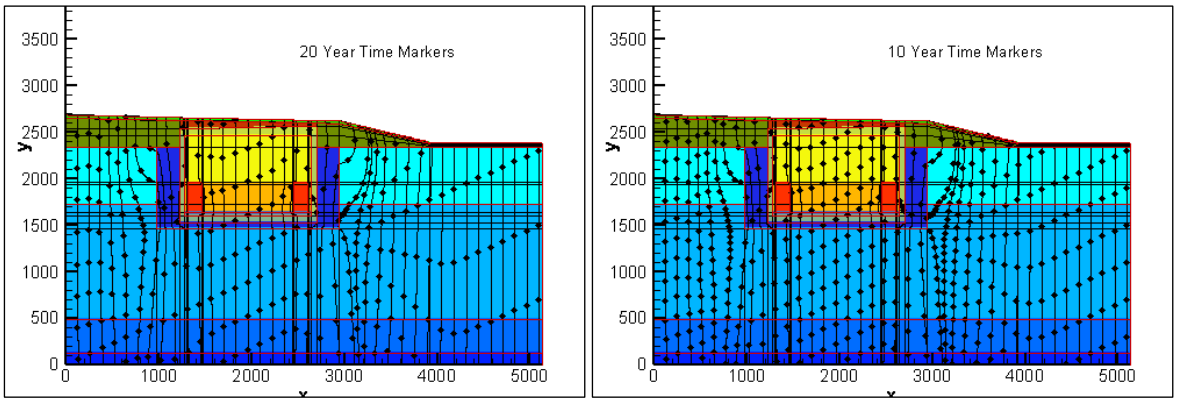

Figure 6-7 Flow field in 4 TPBAR ILV model: (1620 – 1770) and (1920 – 2070) years.

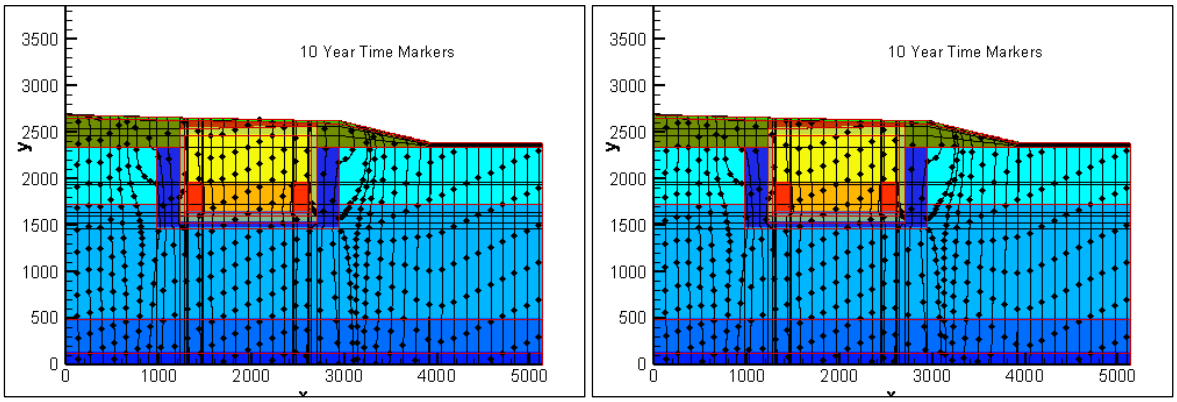

Figure 6-8 Flow field in 4 TPBAR ILV model: (2220 – 2370) and (2520 – 2670) years.

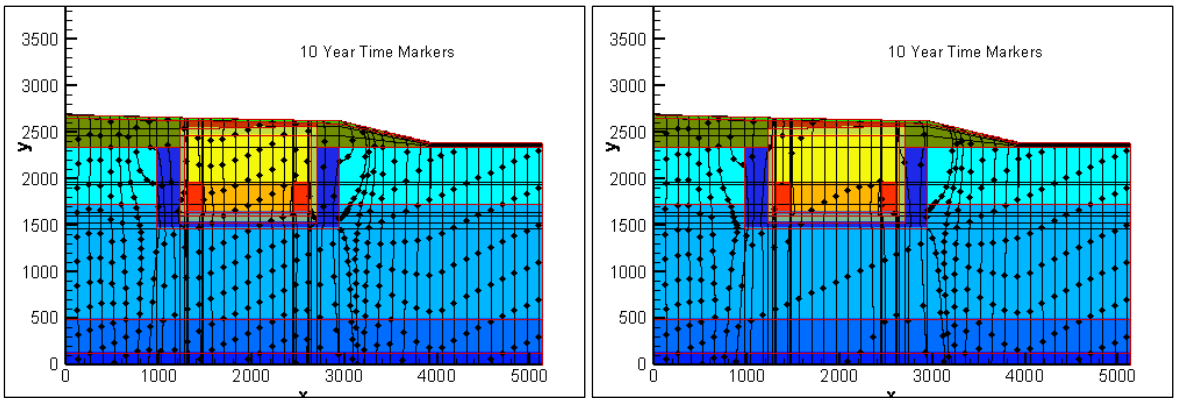

Figure 6-9 Flow field in 4 TPBAR ILV model: (2820 – 3370) and (5770) years.

6.2 Radionuclide Vadose Zone Transport

ILV model transport calculations were made for the following parent radionuclides and daughters: H-3, C-14, Cl-36, I-129, Ra-226 (Pb-210), and U-234 (Th-230, Ra-226, Pb-210). These radionuclides were chosen as those giving a significant dose and having relatively small disposal limits in the 2008 PA. I-129 is a very useful radionuclide to include to test transport behavior since it has both a long half-life and small K_d. This combination of properties ensures that the I-129 peak will be observed and that the area under the peak should equal the amount initially deposited.

One mole (mol) of each parent radionuclide was distributed uniformly in the waste zone and the resulting flux to the water table (mol/yr) calculated over a 50,000-year period. The parent radionuclide was introduced at the start of ILV operations. Fluxes calculated with all three ILV models are very similar and the model having four TPBAR disposal containers is used as a nominal case to illustrate the results. Because of the impermeable nature of TPBAR containers they are represented in the model as no-flow zones with flow moving around the computational mesh assigned to the containers (about 8.3% of the ILV interior space). At 5770 years, when the ILV roof is assumed to collapse, the existing waste inventory is relocated to the lower 10 feet of the waste zone. This is intended to mimic the consolidation of waste containers within the collapsed vault.

6.2.1 K_d Values

Solid-Liquid distribution coefficients (K_d) were obtained from the latest chemistry data package (Kaplan, 2016). As specified in Section 5.4 Table 9 of the data package, reducing cement K_d values were assigned to ILV slag-based concrete vault and oxidizing cement K_d values assigned to the waste zone due to the intimate contact between encapsulating grout or CLSM and waste containers. The data package also recommended using K_d values impacted by cementitious leachate in the upper and lower vadose zone soils. However, it was decided that a more realistic application of cementitious leachate K_d values would be in the ILV control-compacted soil backfill region which is in immediate contact with vault concrete (see Figure 5-5). The 2008 PA model did not use cementitious leachate K_d values in vadose zone soil, so the approach taken in the current modeling is a compromise between the two choices.

6.2.2 Concrete Aging

Concrete K_d values vary as concrete ages (Kaplan, 2016). Concrete aging is related to the number of pore volume exchanges made as water flows through the material. The 2016 chemical data package assumes the following concrete aging:

- Stage I (young) concrete lasts for 50 exchange cycles
- Stage II (middle) concrete lasts for 500 exchange cycles
- Stage III (aged) concrete lasts 4000 exchange cycles

After 4000 pore volume exchanges, concrete K_d values are assumed to become those for clayey soil. For this model assessment, a relatively simple method was used to estimate pore volume exchanges. For the ILV roof and floor and the waste zone, the average vertical velocity during each flow period (Table 5-1) was used to calculate the number of pore volume exchanges. For the ILV walls the average horizontal velocity was used. The cumulative number of pore volume exchanges was tracked through the flow steps and the times calculated when the exchange volumes reached the end of each stage. Table 6-1 gives the resulting times when concrete stage changes occur for

the nominal case. The concrete was aged to the next level at the start of the time step where the number of exchange cycles was reached. Note that the vault concrete and waste zone remained in Stage I throughout the 1000-year post-closure period of performance (170 to 1170 years) except for the vault roof and floor concrete which moved to Stage II at 970 years.

Table 6-1 Estimated ILV Concrete Aging Times in Years

	Roof	Floor	North Wall	South Wall	Waste
Stage I to II	970	970	2070	2070	2220
Stage II to III	1920	2070	5770	5770	5770
Stage III - Soil	5770	5770	5770	5770	5770

The results in Table 6-1 are in reasonably good agreement with the aging times used in the 2008 PA. The 2008 PA aged all ILV concrete from Stage I to Stage II at 1600 years and from Stage II to Stage III at 3800 years. The 2008 PA aged the cementitious waste zone from Stage I to Stage II at 1900 years and from Stage II to Stage III at 3800 years.

6.2.3 Radionuclide Flux to Water Table

Graphs of flux to the water table (mol/yr) for the radionuclides used for this preliminary vadose zone model evaluation are shown in Figure 6-10 through Figure 6-13. Figure 6-13 shows U-234 and its daughters on both a linear and a semi-log scale to include Pb-210. The graphs are for transport from an ILV cell with four TPBAR disposal containers. Table 6-2 compares the maximum flux and the time when the maximum flux occurs for all radionuclides and all three ILV cell configurations. In general, the maximum flux and timing of the maximum are very close for the three different configurations. Concentration profiles showing C-14 transport through the ILV vadose zone at 12 simulation times between 100 and 9900 years are presented in Appendix C.

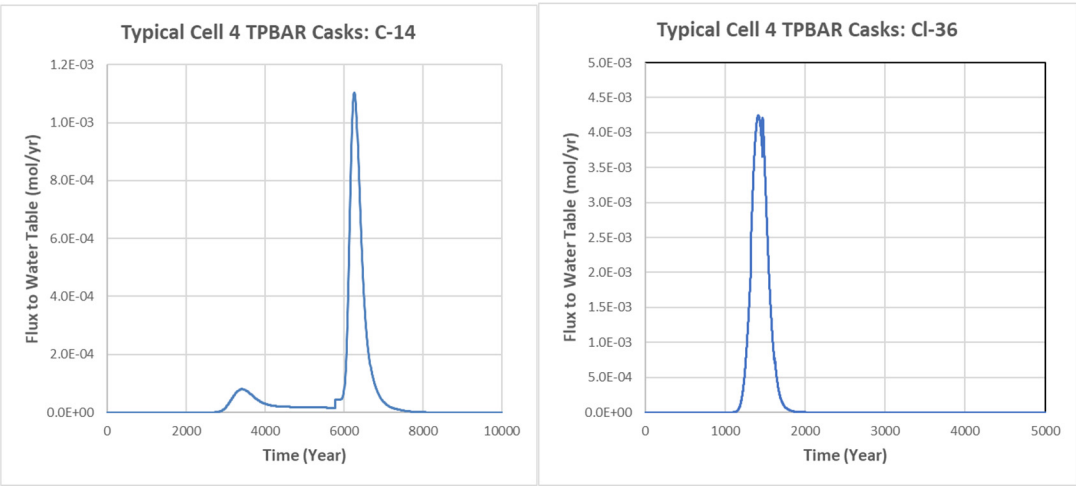

Figure 6-10 Flux to water table for C-14 and Cl-36.

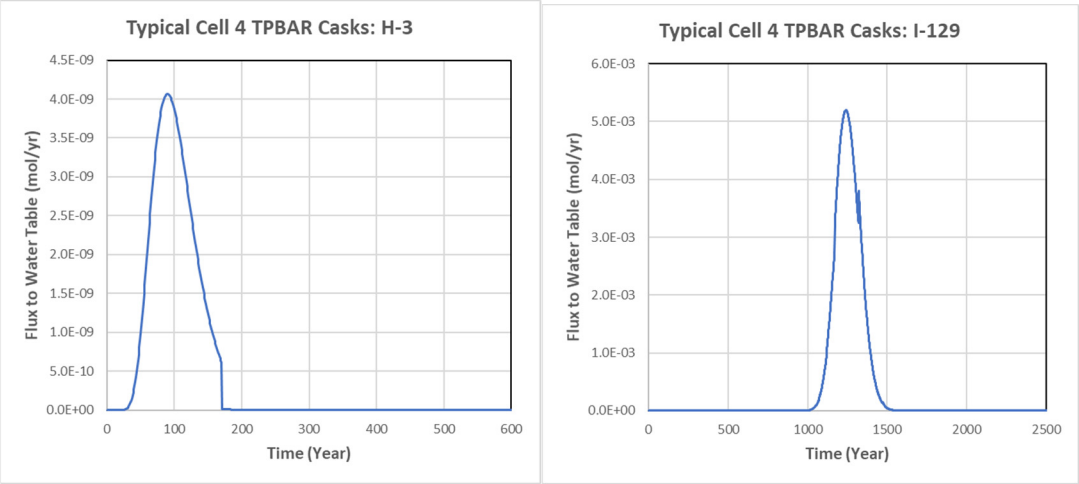

Figure 6-11 Flux to water table for H-3 and I-129.

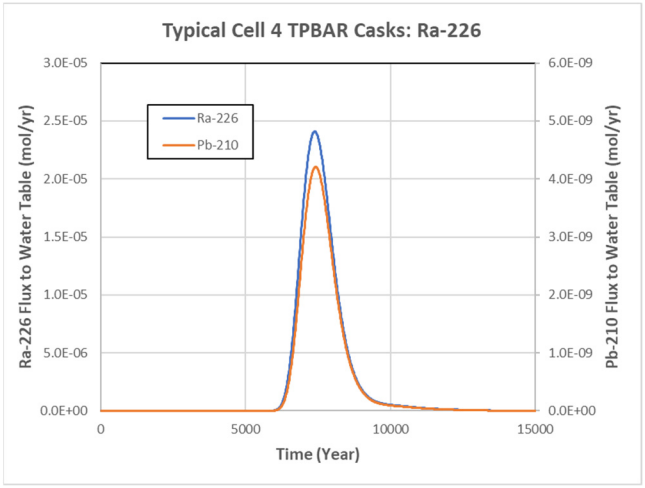

Figure 6-12 Flux to water table for Ra-226 and daughter Pb-210.

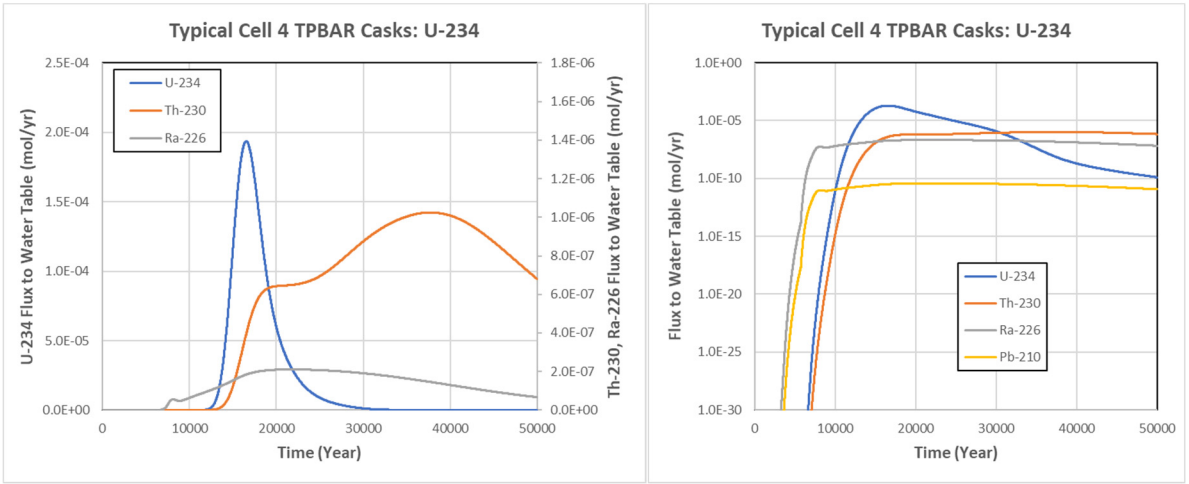

Figure 6-13 Flux to water table for U-234 and daughters Th-230, Ra-226, Pb-210.

Table 6-2 Maximum Flux to Water Table and Time of Maximum Flux for Three ILV Configurations

Nuclide	Center Cell Max mol/yr	Center Cell Year	4 TPBAR Max mol/yr	4 TPBAR Year	8 TPBAR Max mol/yr	8 TPBAR Year
C-14	1.02E-03	6260	1.11E-03	6260	1.20E-03	6240
Cl-36	4.15E-03	1407	4.25E-03	1415	4.30E-03	1471
H-3	4.79E-09	88	4.06E-09	90	4.53E-09	90
I-129	5.07E-03	1237	5.19E-03	1241	5.31E-03	1243
Ra-226	2.48E-05	7410	2.41E-05	7390	2.22E-05	7210
Pb-210	4.32E-09	7440	4.21E-09	7420	3.88E-09	7240
U-234	1.83E-04	16680	1.94E-04	16530	2.01E-04	15890
Th-230	1.03E-06	38500	1.02E-06	37690	9.96E-07	35680
Ra-226	2.10E-07	21920	2.10E-07	21620	2.05E-07	22410
Pb-210	3.67E-11	21950	3.68E-11	21660	3.59E-11	22450

6.2.4 Comparison to 2008 PA

Timeline. In the current ILV model, time zero is the start of ILV operations in 1995 and the end of ELLWF operations is expected to be in 2065. This is a span of 70 years after which the 100-year period of institutional control begins. The 2008 PA calculations assumed that ELLWF operations would end and institutional control begin in 2020 which was chosen to be time zero in the model. An initial time period of -25 years was used in the PA model to account for radionuclide decay and daughter ingrowth following waste disposal at the start of operations in 1995. The additional 45 years of operation in the new PA calculation gives more time for radionuclide decay and daughter ingrowth. However, except for H-3 with a half-life of 12.32 years, the additional time should not make a significant difference in the results. In the comparison of results discussed in this section, results from the 2008 PA and current models are both plotted taking time zero as the start of ILV operations.

Vadose Zone. 60.5 ft depth in 2008 PA model versus 76.5 ft depth in current model. As noted in Section 4, the PORFLOW model used for the 2008 PA did not include the Tan Clay or Lower Aquifer zones.

Infiltration. Figure 6-14 compares the ILV infiltration over the vault used in the 2008 PA with the 2019 calculation (Dyer, 2019) used for the present modeling. Both calculations were made with the HELP model. However, the 2019 infiltration is significantly lower than the 2008 values during the first 2000 years and remains lower until vault roof collapse. Lower infiltration slows the transport of radionuclides through the ILV vadose zone. The biggest change between the 2008 PA and current closure concept is that an HDPE geomembrane liner has been added where the 2008 PA only included a geosynthetic clay liner (GCL). The geomembrane provides the primary barrier to water infiltration in the current HELP results. ILV roof collapse at 5770 years results in a large increase in flow through the vault area assuming runoff from the intact closure cap will enter the cavity created by vault failure and waste subsidence.

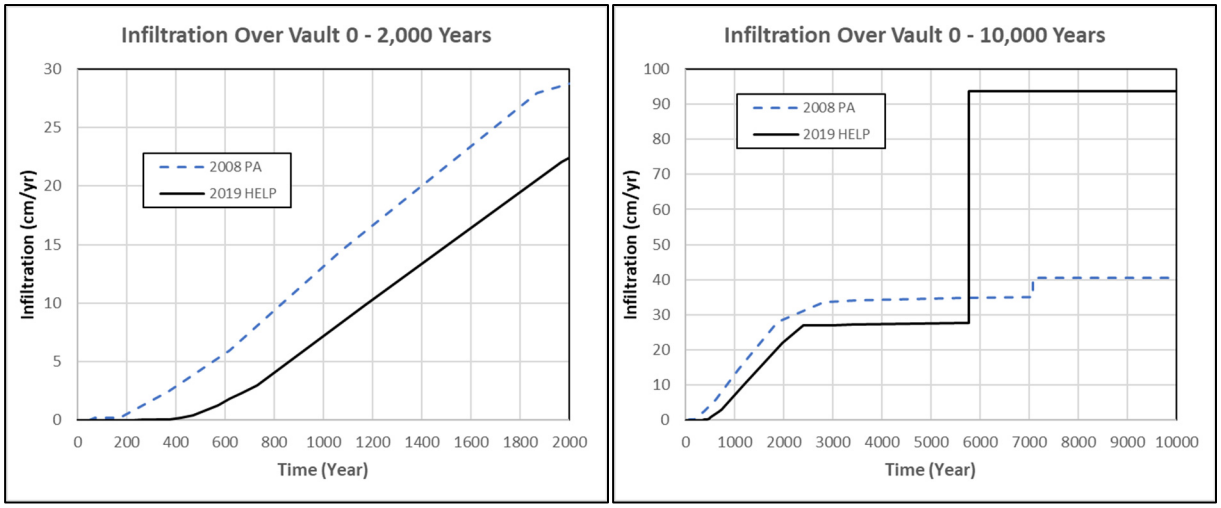

Figure 6-14 Comparison of HELP ILV infiltration for 2008 PA and 2019.

Concrete Degradation. Static load cracks that do not penetrate the concrete are realized within the roof slab and walls as soon as the closure cap is emplaced as documented in the ILV structural analysis (Peregoy 2006). In the 2008 PA, the cracks estimated to exist at 5000 years were utilized to produce an equivalent saturated hydraulic conductivity for the roof slab and side and end walls at the time of closure cap emplacement. A separate simulation of Cell 4 (i.e., center cell) was conducted assuming a fully penetrating crack occurs from a PC-4 seismic event at 400 years. The wall and floor concrete were assigned gravel properties at that time. The structural analysis estimated the probability of a P-4 seismic event to be 39.3% over 5000 years and recommended linear extrapolation to time zero. This implies less than a 4% probability at 400 years.

In the current analysis, surface cracking at the time of closure cap placement is modeled by blending the roof and wall concrete with gravel (90% concrete and 10% gravel). The concrete/gravel mixture is then blended with ILV soil at 50-year increments over the next 500 years. At 400 years the concrete would have the hydraulic properties of 80% soil, 2% gravel, 18% E-Area concrete. Because the choice of 400 years for through-cracking was somewhat arbitrary (choosing an approximate 5% probability of occurrence at 500 years would have also been acceptable), the current analysis did not include the change of wall and roof hydraulic properties to gravel at 400 years but simply continued the concrete degradation between 400 and 500 years. Both models transitioned to soil properties for the entire vault concrete at 500 years.

Sorption Properties. Significant differences in sorption properties found for the radionuclides included in this study are summarized in Table 6-3. While there are significant differences in Ra-226 and Pb-210 K_d values, a comparison for these radionuclides was still made.

Table 6-3 Sorption Properties in Current ILV Model and 2008 PA Version

Current Model		2008 PA Model		Impact on Transport
C-14 K_d sand = 5, K_d clay = 150 Solubility: RC-I and OC-I = 10^{-5} mol/L RC-II and OC-II = 10^{-6} mol/L		**C-14** K_d sand = 0, K_d clay = 0 Solubility: RC-I and OC-I = 10^{-6} mol/L RD-II and OC-II = 10^{-4} mol/L		C-14 released earlier in 2008 PA model.
Ra-226 K_d: sand 25 clay 180 [1]RC-I 6000 [2]RC-II 600 [3]OC-I 200 [4]OC-II 200	**Pb-210 K_d**: sand 2000 clay 5000 [1]RC-I 5000 [2]RC-II 1000 [3]OC-I 300 [4]OC-II 100	**Ra-226 K_d**: sand 5 clay 17 [1]RC-I 100 [2]RC-II 70 [3]OC-I 100 [4]OC-II 70	**Pb-210 K_d**: sand 5 clay 5000 [1]RC-I 500 [2]RC-II 250 [3]OC-I 500 [4]OC-II 250	Transport of Ra-226 and Pb-210 reduced in current model except for Pb within the waste zone where K_d's are reduced.

[1]Reducing concrete Stage I: ILV concrete [3]Oxidizing concrete Stage I: waste
[2]Reducing concrete Stage II: ILV concrete [4]Oxidizing concrete Stage II: waste

Results. Comparison of fluxes to the water table for six parent radionuclides and daughters are shown in Figure 6-15 through Figure 6-17. All radionuclide releases are assumed to be K_d controlled.

The peak flux for C-14 in Figure 6-15 occurs shortly after ILV roof collapse in both models (1900 years and 5770 years). The C-14 peak in the current model is 24% of the 2008 PA peak both because of peak spreading and the longer retention time of approximately one half-life in the current model. As shown in Table 6-3, there are significant differences in both C-14 K_d and solubility between the two models.

The peak flux for Cl-36 in Figure 6-15, which occurs after concrete degradation is complete, appears sooner in the current ILV model than in the 2008 PA version. This is likely a result of faster transport through the degraded ILV concrete. The peak flux in the current model is only 13% of the 2008 PA value. As with C-14, the 2008 PA flux is very high and narrow occurring almost immediately after roof collapse. This sudden flushing of the radionuclide from the vadose zone following roof collapse tends to cause these higher and narrower flux peaks. Although, the Cl-36 peak flux in the current model is much smaller than in the 2008 PA version, it occurs closer to the compliance period and consequently may be more conservative.

The peak H-3 flux shown in Figure 6-16, which appears well before concrete degradation starts, is 84% higher in the current model. The I-129 flux in Figure 6-16 is 16% higher than the 2008 PA value which is the closest comparison obtained between the two models. Occurring sooner in the new model it may adversely impact limits during the compliance period.

Fluxes to the water table for Ra-226, U-234 and the U-234 daughters are presented in Figure 6-17. As shown in Table 6-3, K_d values for Ra-226 and Pb-210 are much different in the latest chemical data package and the Ra-226 curve has peaked further out in time in the current model and is much

smaller. Qualitatively U-234 and daughter fluxes compare relatively well with all peak fluxes occurring after about 20,000 years, well beyond the compliance period. The Ra-226 release from U-234 decay in the 2008 PA extends back to about 1000 years and is likely the cause of groundwater pathway U-234 disposal limits.

The 2008 PA peak fluxes for C-14, Cl-36, I-129 and Ra-226 all appear at 1900 years when infiltration flow increases from ILV roof collapse. The choice of 1900 years for roof collapse was somewhat arbitrary and creates abnormally sharp peaks for these radionuclides. The increased K_d values for C-14, Ra-226 and Pb-210 shown in Table 6-3 cause fluxes to the water table for these radionuclides to peak later in the current model which should significantly increase groundwater pathway disposal limits for these radionuclides.

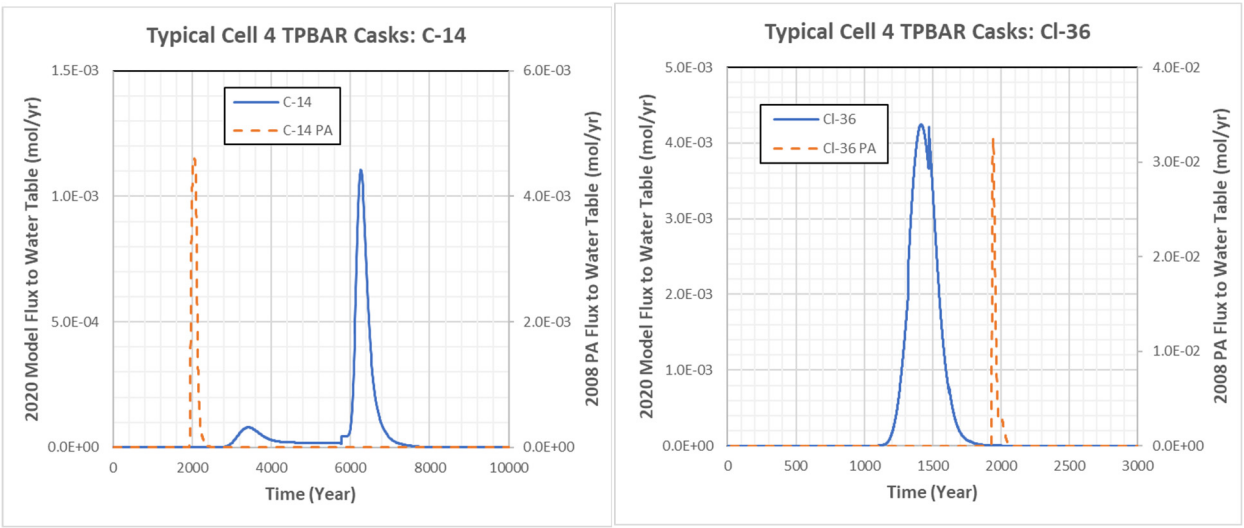

Figure 6-15 Flux to water table for C-14 and Cl-36 in current and PA models.

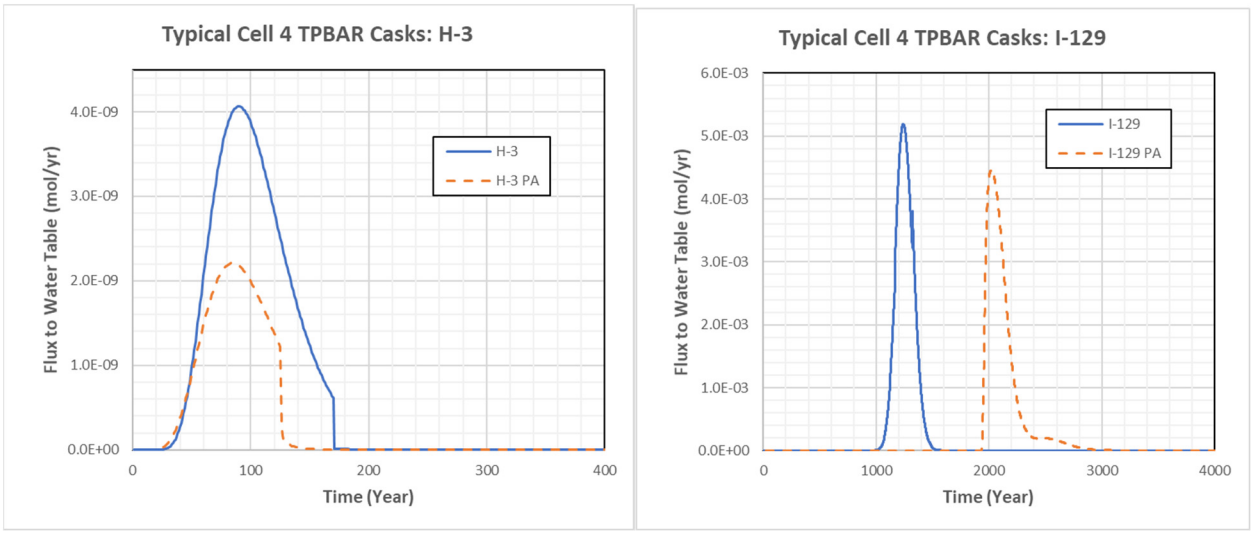

Figure 6-16 Flux to water table for H-3 and I-129 in current and PA models.

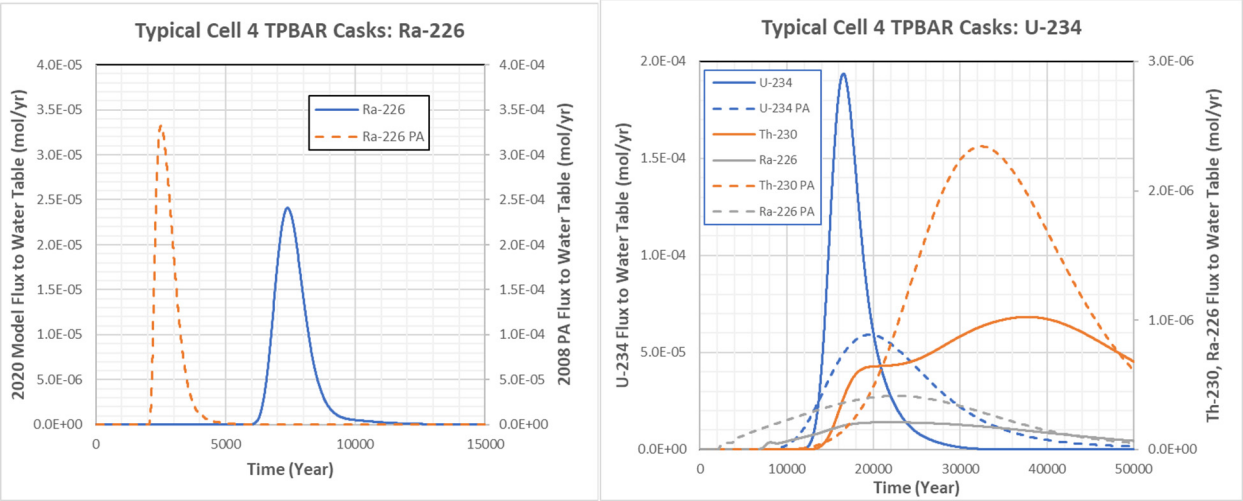

Figure 6-17 Flux to water table for Ra-226 and U-234 in current and PA models.

6.3 TPBAR Tritium Release

The only special waste forms evaluated in testing the ILV vadose zone model were the release of tritium and argon-39 from TPBAR disposal containers. Analysis of TPBAR tritium is described in this section and TPBAR argon-39 is discussed in Section 6.4. In the 2008 PA, it was assumed that the 17 TPBAR disposal containers expected to be sent to ILV were simultaneously buried at the end of operations which was then expected to occur in 2020. It was also assumed that the containers would be placed within ILV cells in two stacks of two containers each, near the outer walls, as shown in Figure 5-3. The 2008 PA and a related Special Analysis (Hiergesell, 2005) used an unclassified tritium release rate calculated by Pacific Northwest National Laboratory (PNNL). The release rate for a single disposal container is provided in Section 5, Table 3 of the SA (Hiergesell, 2005). The single container release rate was multiplied by the number of containers that would be disposed in the ILV and the total release used as a source term in the PORFLOW model. The release was modeled as occurring directly into a "halo" region surrounding the disposal containers.

Solid Waste currently expects to place 28 TPBAR disposal containers in the ILV. The expected release of tritium from TPBAR disposal containers has also been recalculated by SRNL (Gorensek, 2021). The current TPBAR modeling follows the 2008 PA approach of releasing the tritium into a 6-inch region around each stack of disposal containers. The release region is above and on either side of the stacks. The stacks are placed one foot from the wall and the region surrounding the stacks, including the tritium release zone, are located within the cell waste zone. The updated calculation revised the 2008 PA approach by timing tritium release to follow the expected TPBAR disposal schedule shown in Table 6-4 and using the SRNL release rate. The new modeling further assumes that the first 12 TPBAR disposal containers will be placed in three ILV cells with four containers per cell while the last 16 TPBAR disposal containers will be placed in two ILV cells with eight containers per cell. The later disposal configuration is shown in Figure 5-4.

The SRNL analysis considered four cases:

1. One-year old TPBAR disposal containers, eight per ILV cell
2. Five-year old TPBAR disposal containers, eight per ILV cell
3. One-year old TPBAR disposal containers, four per ILV cell
4. Five-year old TPBAR disposal containers, four per ILV cel1

The first and third cases, which released the most total tritium (6507 Ci and 3279 Ci, respectively), were used in the modeling. Figure 6-18 shows tritium flux to the water table from the 2008 PA and current ILV model. Time zero in this figure is 1995 the approximate start of ILV operations. The total peak flux to the water table in the revised calculation is about 82% of the 2008 PA value. Even though the revised calculation assumes 28 disposal containers instead of 17, the combination of using a more realistic disposal schedule, which spreads the release out over time, and the revised estimate of tritium release produced a slightly lower peak flux. Therefore, it is expected that TPBAR disposal limits will remain approximately the same in the revised PA.

Table 6-4 Schedule for Dispositioning TPBAR Disposal Containers (TDC)

Year	TDC	Year	TDC	Year	TDC
2009	1	2023	2	2029	2
2015	1	2024	1	2030	1
2017	1	2025	1	2031	2
2020	2	2026	2	2032	2
2021	1	2027	2	2033	2
2022	1	2028	2	2034	2

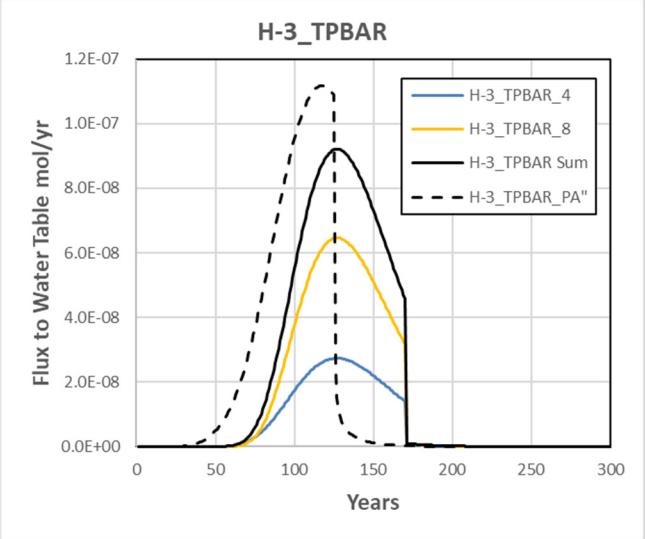

Figure 6-18 Tritium flux to water table from TPBAR disposal containers.

6.4 TPBAR Argon-39 Release

Argon as Ar-39 may also be released from TPBAR disposal containers. As a conservative approach, a release rate was calculated (Gorensek, 2021) assuming that one Curie of Ar-39 instantaneously enters the void volume in a TPBAR cask at the time of disposal. The Ar-39 is then released from the cask into the ILV waste zone at the maximum allowed disposal container leak rate. The ILV Vadose Zone PORFLOW model was used to calculate the resulting Ar-39 flux to the water table.

Figure 6-19, compares flux to water table from 1.0 Ci generic Ar-39 and 1.0 Ci Ar-39 released from TPBAR disposal containers. At the peak, the TPBAR Ar-39 flux is about 1/8 of the generic value. The TPBAR SA (Hiergesell, 2005) gives an inventory of 193 Ci Ar-39 for 17 TPBAR disposal containers which scales up to 318 Ci for 28 TPBAR casks. Chapter 8, Table H-57 in the 2022 PA gives a disposal limit for ILV generic Ar-39 of 1.12E+06 Ci. Applying the generic disposal limit to include Ar-39 present in TPBAR casks is therefore conservative and, by a large margin, exceeds any expected Ar-39 disposal in the ILV.

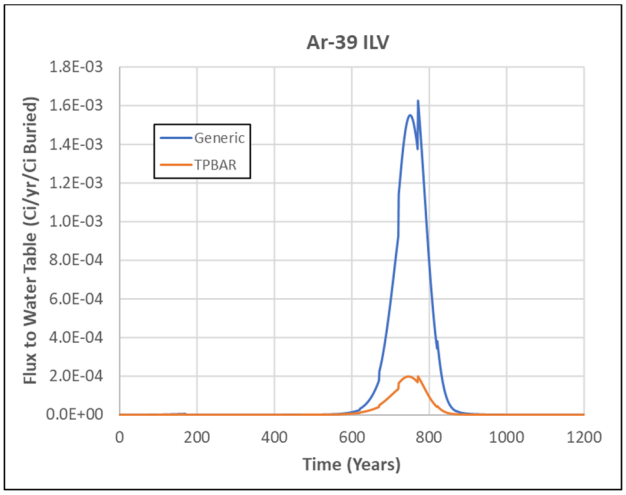

Figure 6-19 Flux to the water table from the release of 1.0 Ci Generic Ar-39 and 1.0 Ci TPBAR Ar-39.

7.0 Conclusions

This report describes the development and testing of a PORFLOW model to calculate water flow and radionuclide transport through the E-Area ILV and its associated vadose zone. The model is geometrically very similar to the model used for the 2008 E-Area PA. Improvements made to the previous model include:

- A refined computational mesh encompassing a larger area.
- Implementation of a novel method to estimate degradation of concrete hydraulic properties.
- Including the soil cover over the ILV in the model.
- Revised vadose zone structure.
- Revised infiltration rates.
- Updated material properties.
- Updated solid-liquid distribution coefficients.
- Updated schedule for disposition of TPBAR disposal containers and updated tritium release.

Results for all flow calculations required to perform the next PA and for trial radionuclide transport calculations are presented in the report. A trial calculation for nominal TPBAR disposal conditions is also included. For TPBAR transport, the tritium release was based on the proposed disposal schedule instead of assuming simultaneous disposal of all TPBAR inventory. While all the radionuclide transport results appear to be reasonable, hydraulic degradation of the vault concrete and reduced infiltration rates lead to some of the fluxes to the water table peaking close to the 1000 year period of performance. This may cause some PA disposal limits to decrease.

8.0 References

Bagwell, L.A., and P.L. Bennett, 2017. *Elevation of Water Table and Various Stratigraphic Surfaces Beneath E-Area Low Level Waste Disposal Facility*, SRNL-STI-2017-00301, Revision 1, November 2017.

Dyer, J. A., 2019. *Infiltration Data Package for the E-Area Low-Level Waste Facility Performance Assessment*, SRNL-STI-2019-00363, Revision 0, November 2019.

Flach, G. P., 2017. *Method for Modeling the Gradual Physical Degradation of a Porous Material*, SRNL-STI-2017-00525, Revision 0, September 20, 2017.

Gorensek, M. B., 2021, *Updated Estimate of Tritium Permeation from TPBAR Disposal Containers in ILV*, SRNL-STI-2020-00298, Revision 1, November, 2021..

Hiergesell, R. A., 2005. *Special Analysis: Production TPBAR Waste Container Disposal within the Intermediate Level Vault*, WSRC-TR-2005-00531, Revision 0, December 2005.

Kaplan, D. I., 2016. *Geochemical Data Package for Performance Assessment Calculations Related to the Savannah River Site, SRNL-STI-2009-00473*, Revision 1, July 22, 2016.

Nichols, R. L., and B. T. Butcher, 2020. *Hydraulic Properties Data Package for the E-Area Soils, Cementitious Materials, and Waste Zones – Update*, SRNL-STI-2019-00355, Revision 1, May 2020.

Peregoy, W., 2006. *Structural Evaluation of Intermediate Level Waste Storage Vaults for Long-Term Behavior*. T-CLC-E-00024, Revision 0, Washington Savannah River Company, Aiken, SC.

WSRC, 2008. *E-Area Low-Level Waste Facility DOE 435.1 Performance Assessment, Chapter 4 Intermediate Level Vault,* WSRC-STI-2007-00306, Revision 0, July 2008.

C-CT-E-00084, 2016. *Preliminary E-Area Low Level Waste Facility (ELLWF) Conceptual Closure Cap – Details*, Sheet 1 of 4, Revision A, Savannah River Nuclear Solutions, Aiken, SC.

Appendix A: Pressure Distribution in PORFLOW ILV Model

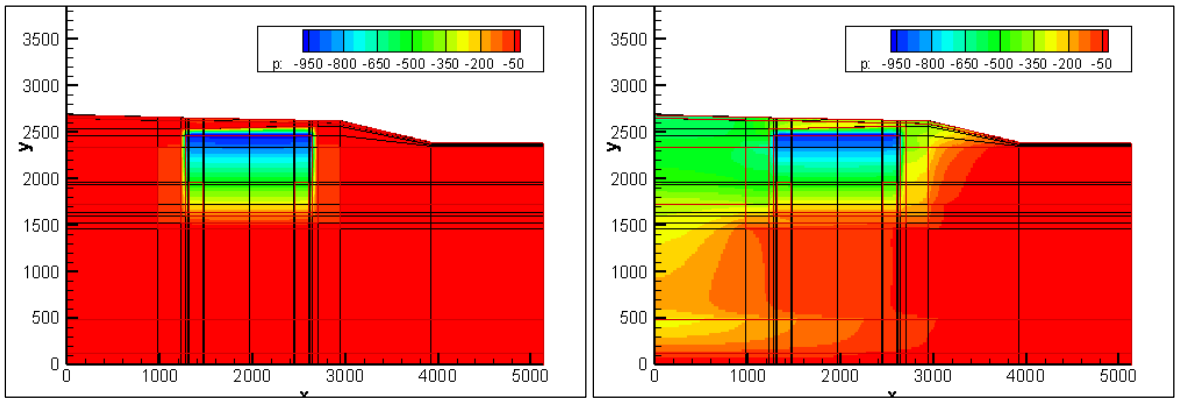

Figure A-1 Pressure in 4 TPBAR model: (0 – 170) and (220 – 270) years.

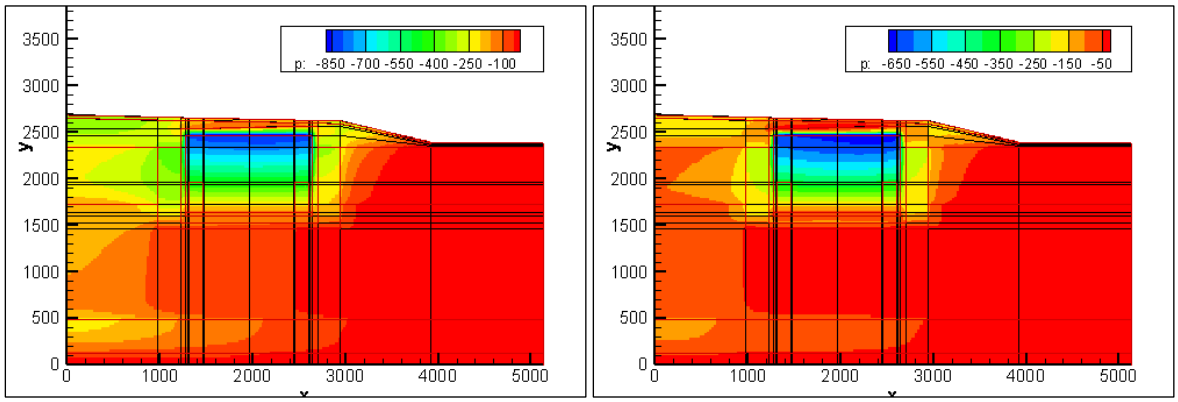

Figure A-2 Pressure in 4 TPBAR model: (320 – 370) and (420 – 470) years.

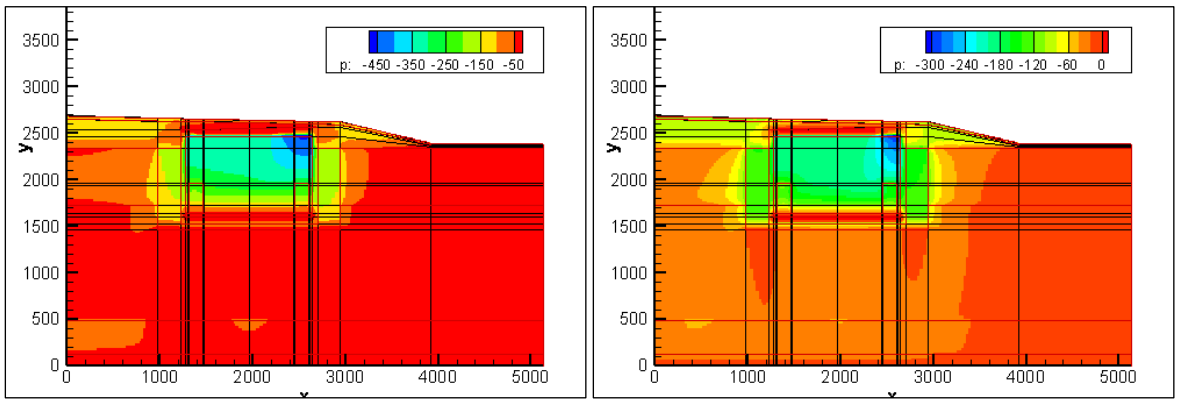

Figure A-3 Pressure in 4 TPBAR model: (520 – 570) and (620 – 670) years.

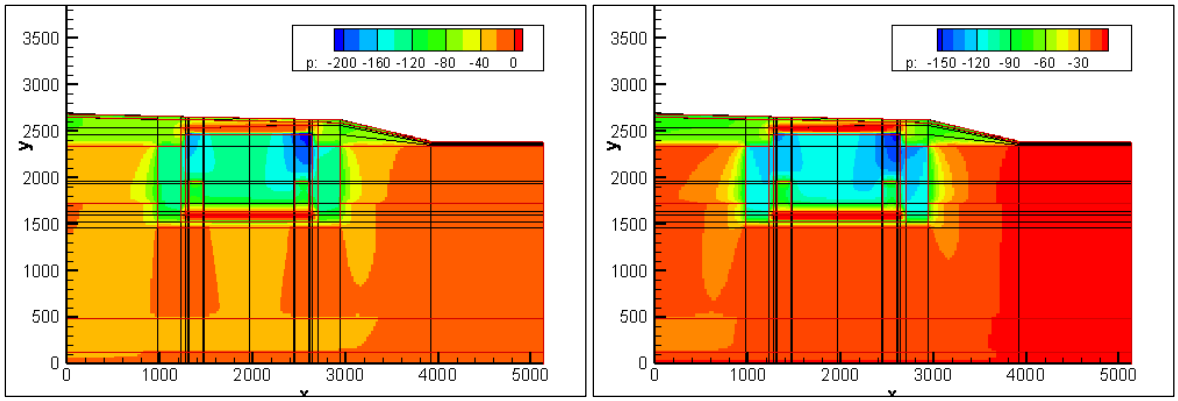

Figure A-4 Pressure in 4 TPBAR model: (720 – 770) and (820 – 870) years.

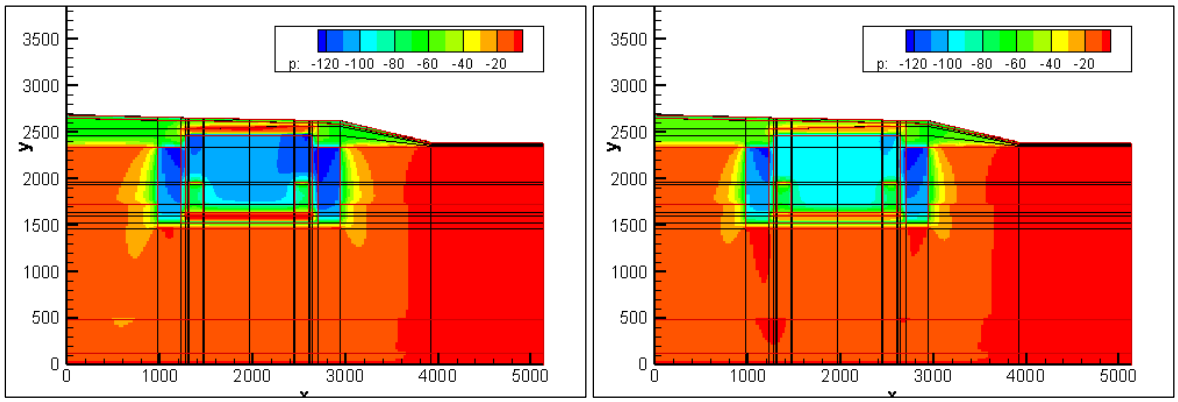

Figure A-5 Pressure in 4 TPBAR model: (920 – 970) and (1020 – 1070) years.

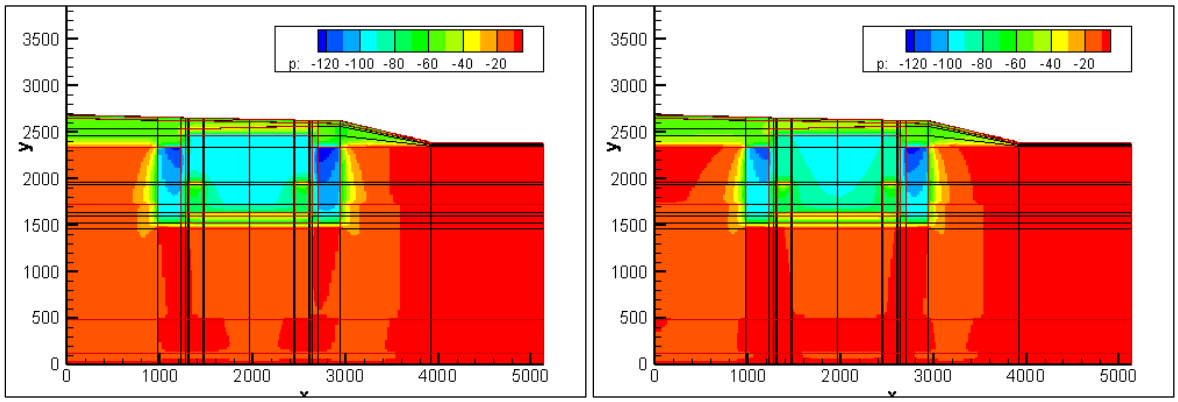

Figure A-6 Pressure in 4 TPBAR model: (1120 – 1170) and (1320 – 1470) years.

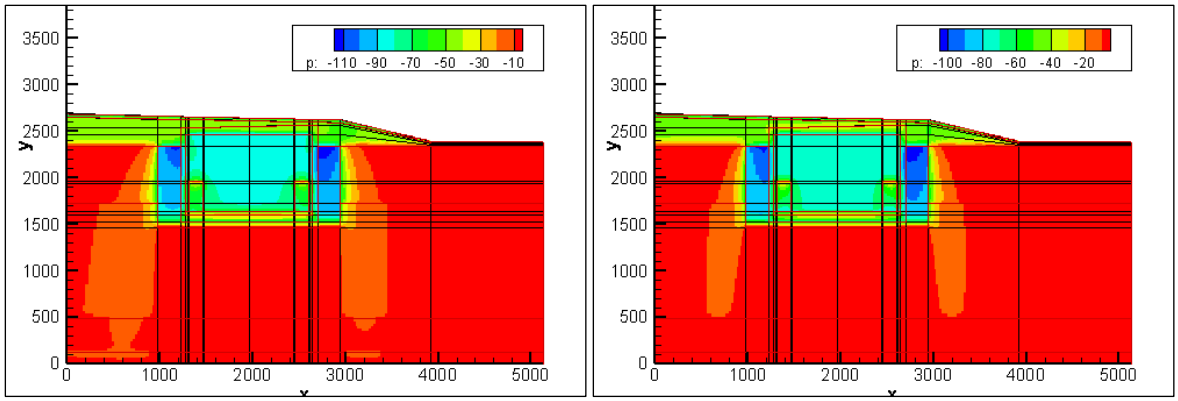

Figure A-7 Pressure in 4 TPBAR ILV model: (1620 – 1770) and (1920 – 2070) years.

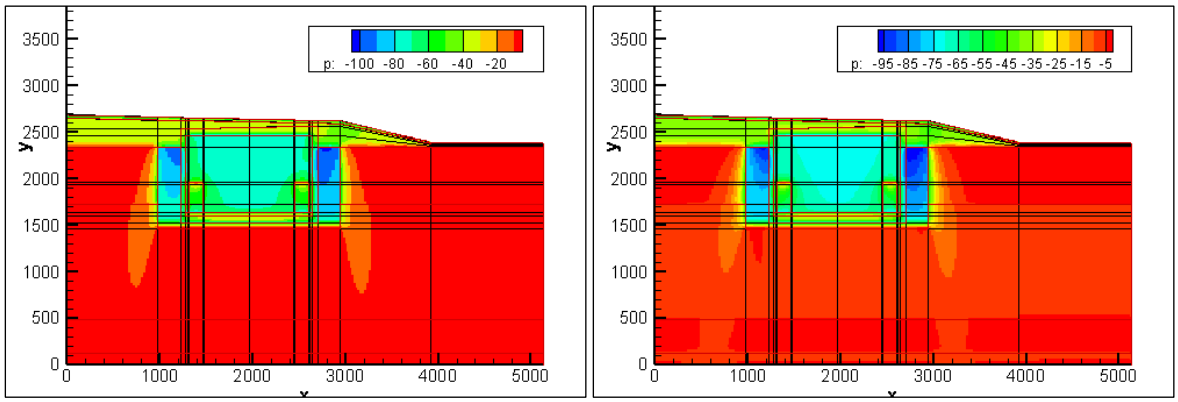

Figure A-8 Pressure in 4 TPBAR ILV model: (2220 – 2370) and (2520 – 2670) years.

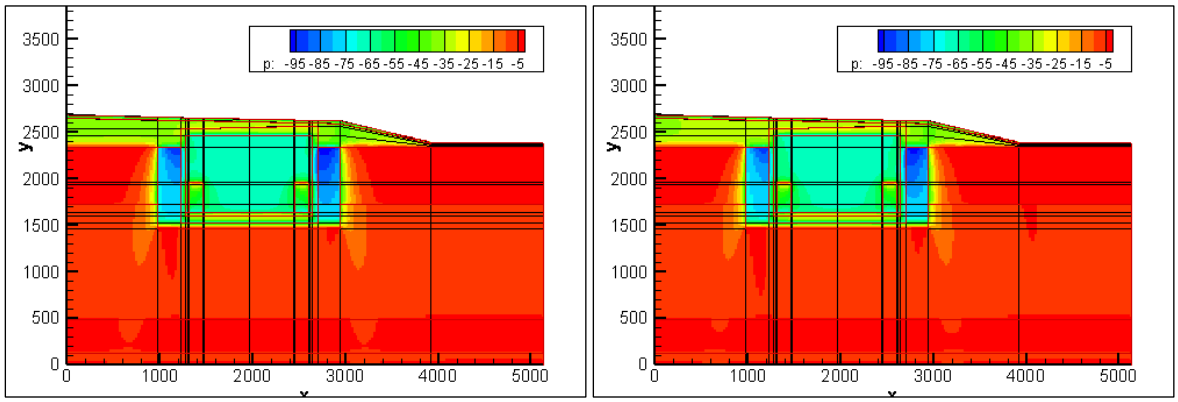

Figure A-9 Pressure in 4 TPBAR ILV model: (2820 – 3370) and (5770) years.

Appendix B: Water Saturation in PORFLOW ILV Model

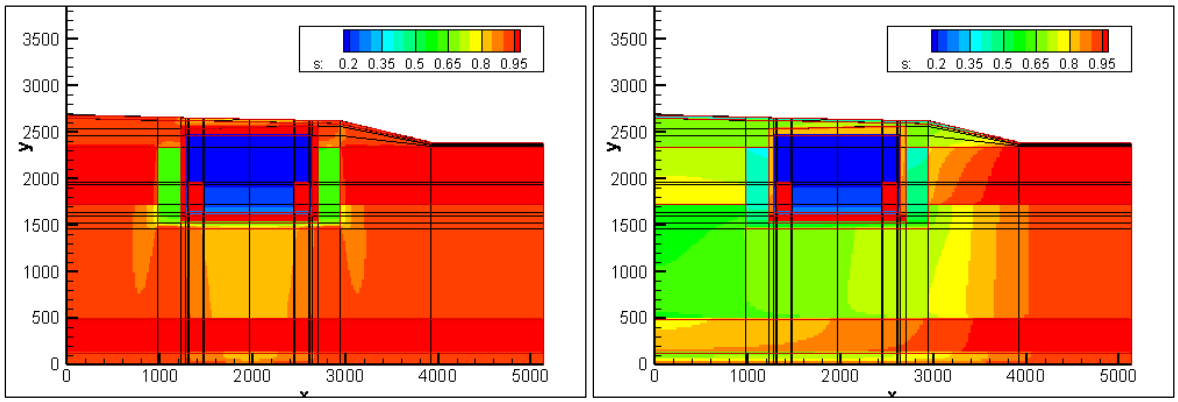

Figure B-1 Saturation in 4 TPBAR model: (0 – 170) and (220 – 270) years.

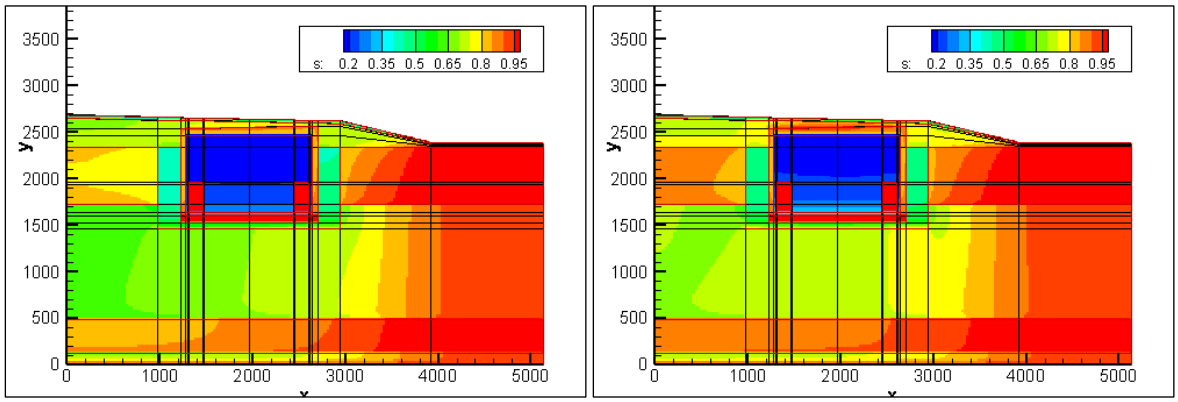

Figure B-2 Saturation in 4 TPBAR model: (320 – 370) and (420 – 470) years.

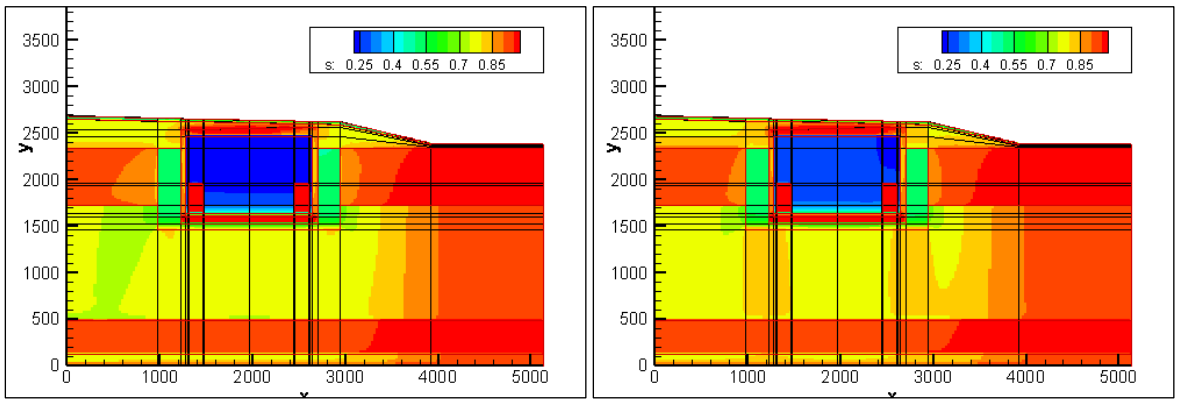

Figure B-3 Saturation in 4 TPBAR model: (520 – 570) and (620 – 670) years.

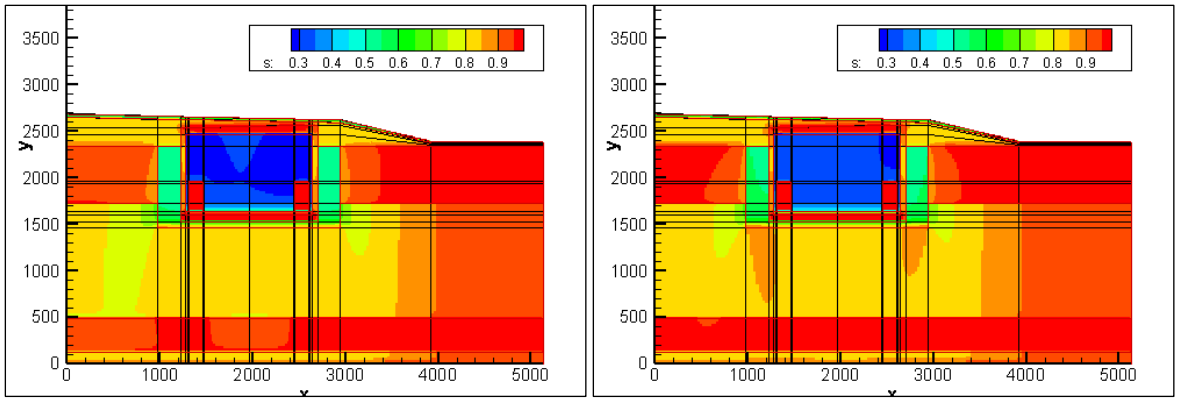

Figure B-4 Saturation in 4 TPBAR model: (720 – 770) and (820 – 870) years.

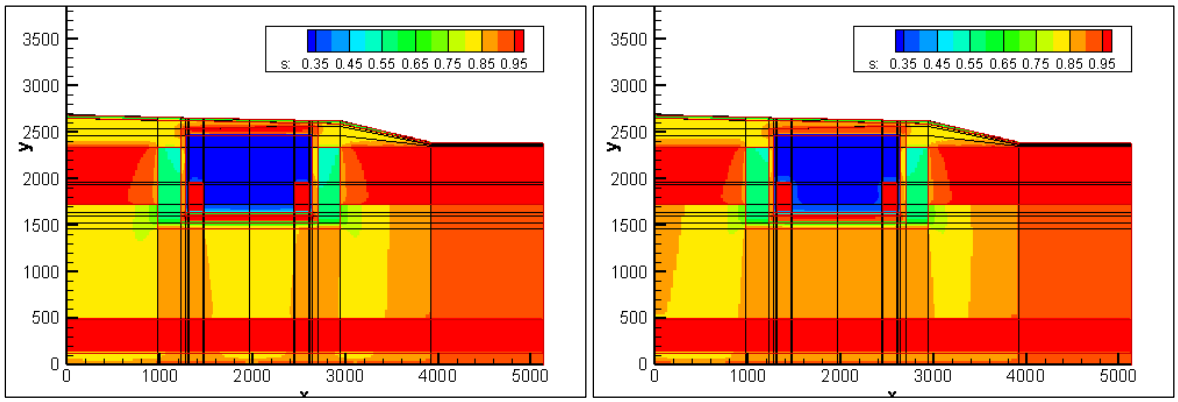

Figure B-5 Saturation in 4 TPBAR model: (920 – 970) and (1020 – 1070) years.

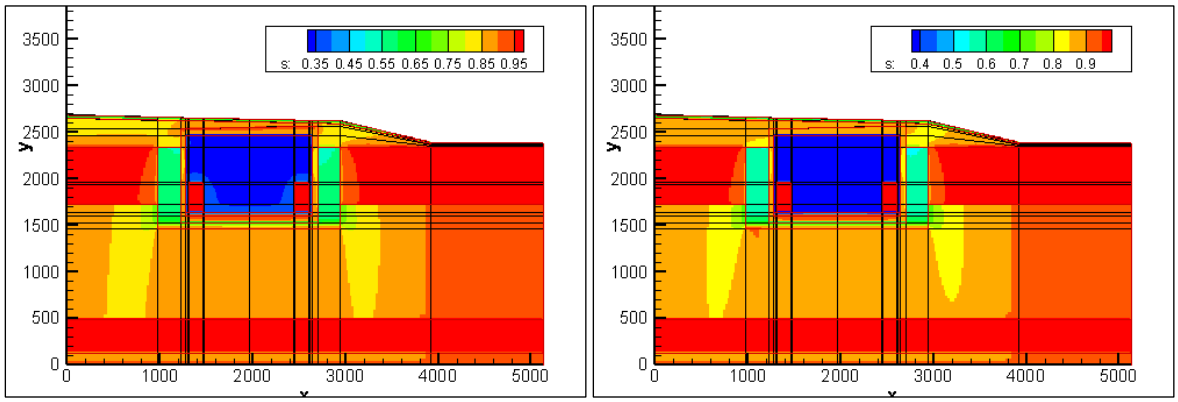

Figure B-6 Saturation in 4 TPBAR model: (1120 – 1170) and (1320 – 1470) years.

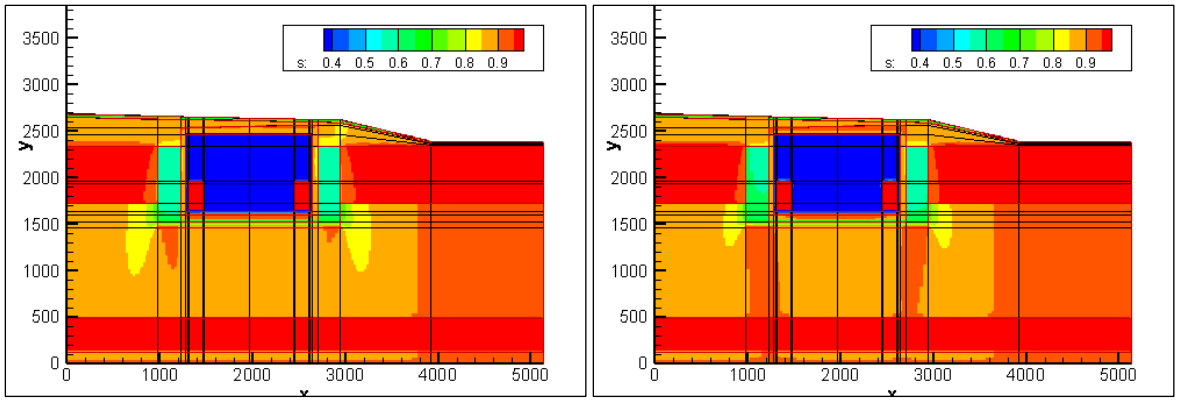

Figure B-7 Saturation in 4 TPBAR ILV model: (1620 – 1770) and (1920 – 2070) years.

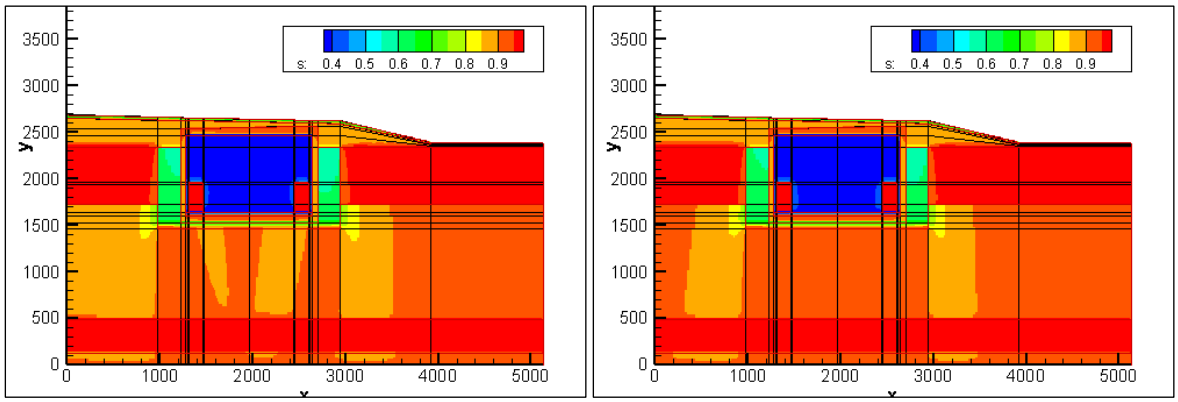

Figure B-8 Saturation in 4 TPBAR ILV model: (2220 – 2370) and (2520 – 2670) years.

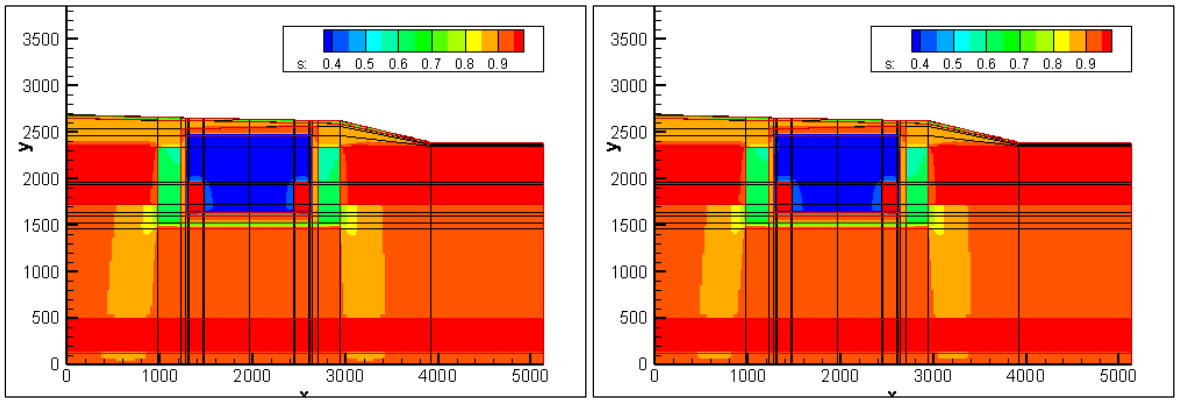

Figure B-9 Saturation in 4 TPBAR ILV model: (2820 – 3370) and (5770) years.

Appendix C: C-14 Concentration Profiles in PORFLOW 4 TPBAR ILV Model

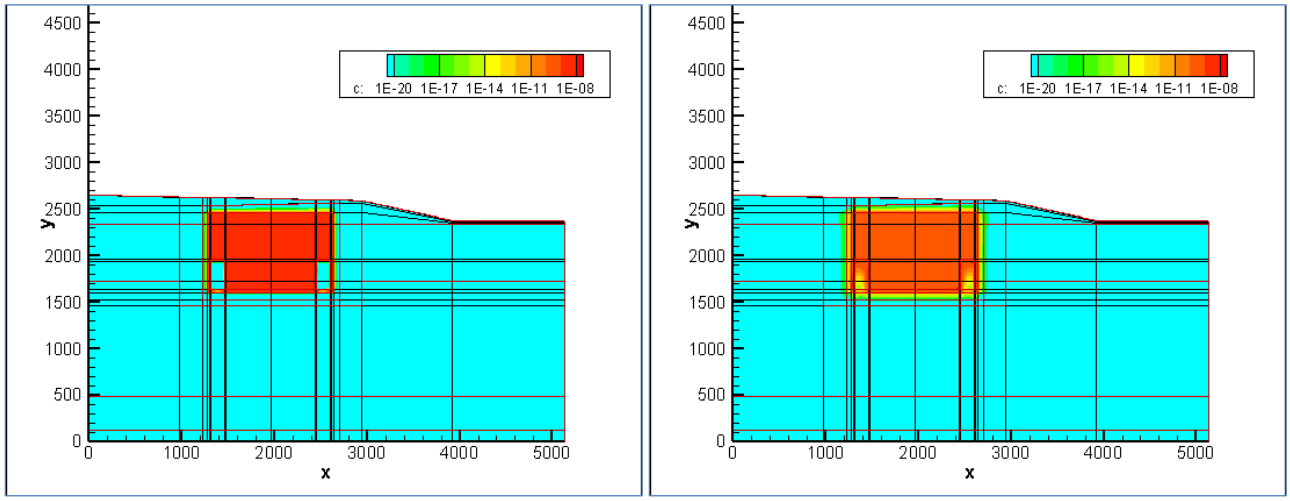

Figure C-1 C-14 Concentration profiles at 100 and 1000 years.

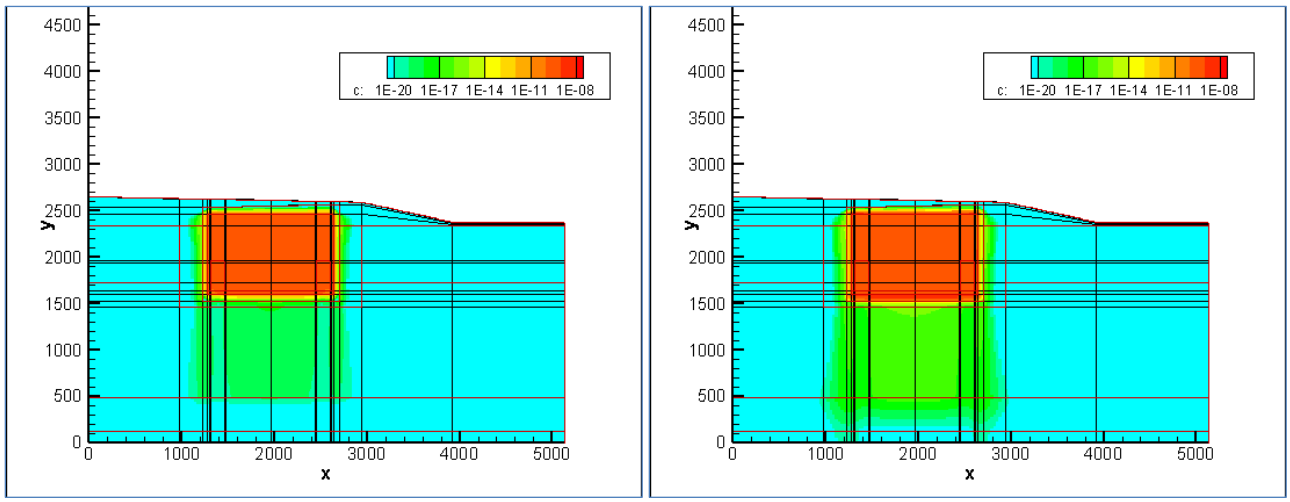

Figure C-2 C-14 Concentration profiles at 1500 and 2000 years.

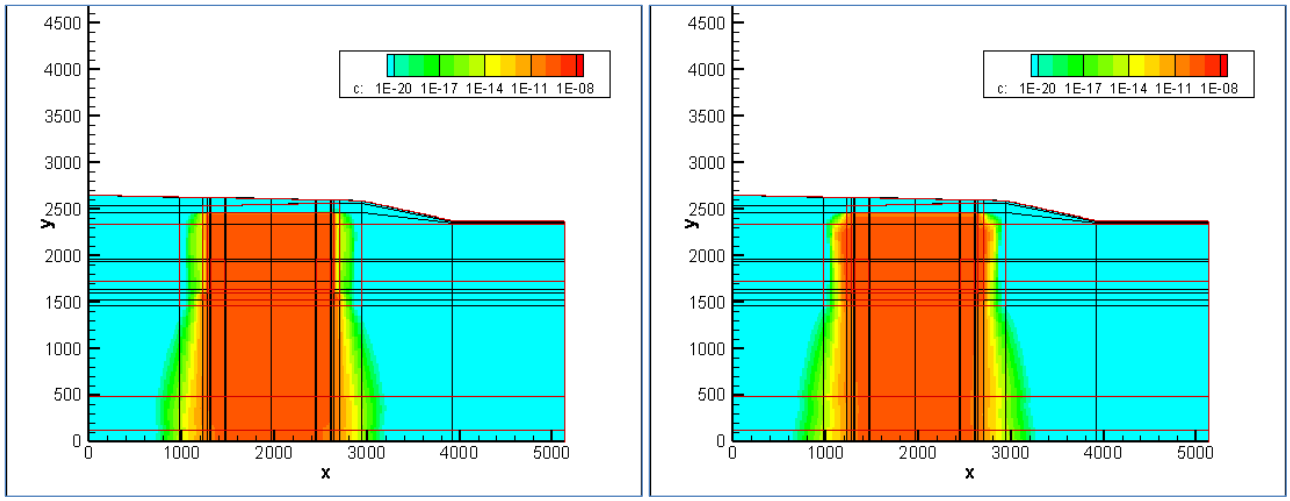

Figure C-3 C-14 Concentration profiles at 3000 and 4000 years.

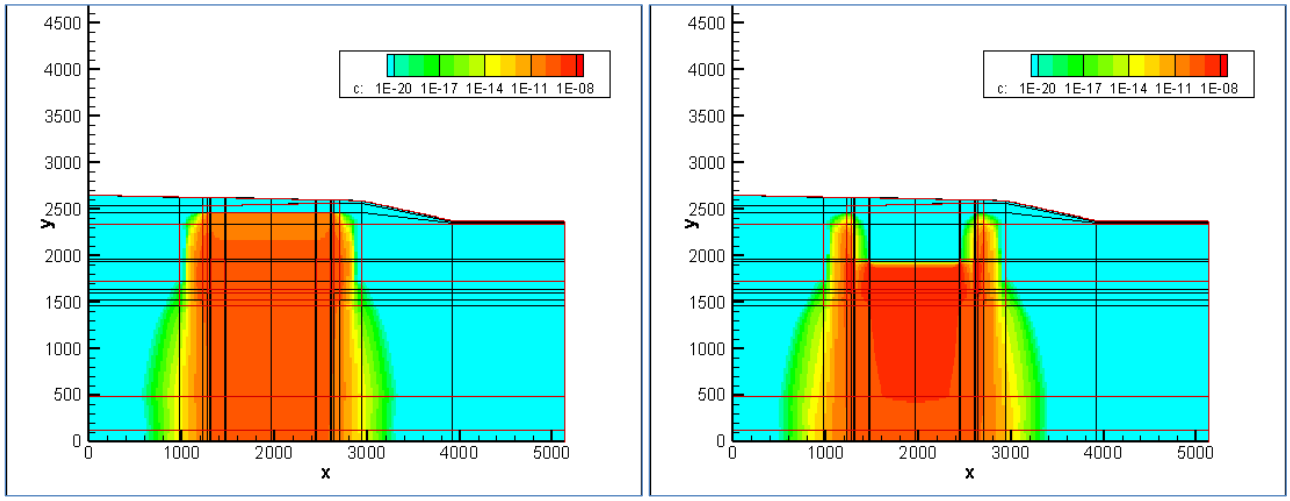

Figure C-4 C-14 Concentration profiles at 5000 and 6000 years.

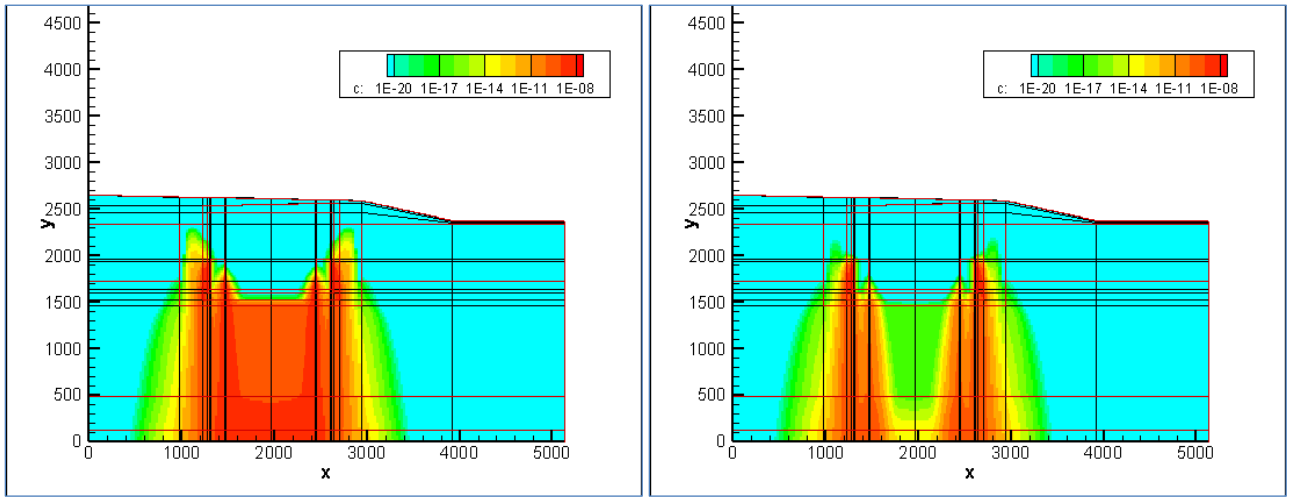

Figure C-5 C-14 Concentration profiles at 7000 and 8000 years.

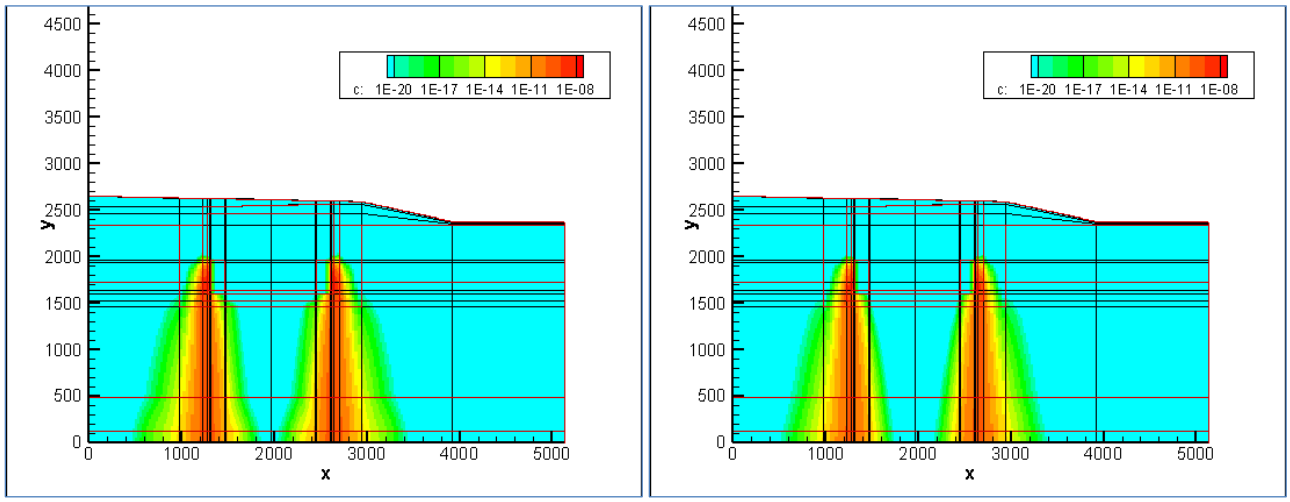

Figure C-6 C-14 Concentration profiles at 9000 and 9900